Affective bonding explains post-traumatic behavioral development in adult mice

Ray X. Lee[1,2,*], **Greg J. Stephens**[2,3], **Bernd Kuhn**[1]

***For correspondence:** rayxin.lee@oist.jp (RL)

[1]Optical Neuroimaging Unit, Okinawa Institute of Science and Technology (OIST) Graduate University, Okinawa, Japan; [2]Biological Physics Theory Unit, OIST Graduate University, Okinawa, Japan; [3]Department of Physics and Astronomy, Vrije Universiteit Amsterdam, Amsterdam, The Netherlands

Abstract Stress incubation is the developmental process by which the onsets of notable stress reactions are appreciably delayed after their trigger. However, how diverse behavioral differences emerge after a protracted symptom-free period remains a major conceptual challenge. Here we examined and analyzed behavioral development in mice isolated after observing a traumatic event inflicted upon their pair-housed partners. Compared to mice isolated without traumatic experience, fine-scale behavioral analysis showed that anxiety-related reactions gradually increased through isolation. These increases were independent of fear memory. Instead of social avoidance from anxiety, traumatized mice presented long-term reduction of social interest to strangers. These behaviors were not observed if the traumatic event happened to strangers. Additionally, traumatized mice showed rebound responses to their partners after a long separation. Affectional bonding as the single common factor underlies the otherwise independent development of post-traumatic behaviors in our paradigm, suggesting a unitary model of stress incubation in mice.

Introduction

Stress reactions can emerge long after their triggering. Stress incubation describes the time interval following an aversive event during which stress reactions emerge or increase. Since the phenomenon of anxiety and fear incubation was first formulated and summarized [***Diven*** (***1937***)], stress incubation has been assumed to be spontaneous in the sense that the development of behavioral changes is highly determined by internal rather than external causes [***McAllister and McAllister*** (***1967***)].

Stress incubation has received serious clinical and research attention in human psychiatry, especially characterized in the post-traumatic stress disorder (PTSD), one of the most prevalent mental health disorders [***DSM-III*** (***1980***); ***DSM-5*** (***2013***)]. Despite such prevalence, PTSD remains far from understood and controversial [***McFarlane*** (***2010***)]. The debates have even questioned the existence of PTSD [***McHugh and Treisman*** (***2007***); ***Walton et al.*** (***2017***)], due to its diversity, inconsistency, and delayed onset of symptoms even after a protracted symptom-free period [***Andrews et al.*** (***2007***); ***Pai et al.*** (***2017***)]. Although the mechanisms underlying PTSD are not well understood [***Schnyder and Cloitre*** (***2015***)], a core belief shared across various hypotheses is to view PTSD as an association between trauma-induced states such as fear memory, increased anxiety, and social withdrawal [***Ehlers and Clark*** (***2000***); ***Siegmund and Wotjak*** (***2006***); ***Hayes et al.*** (***2012***); ***Zoladz and Diamond*** (***2013***); ***Bryant et al.*** (***2017***)]. In this collective model (Figure 1A), behaviors

slowly change and influence each other during stress incubation until a new, abnormal equilibrium is reached; this is PTSD.

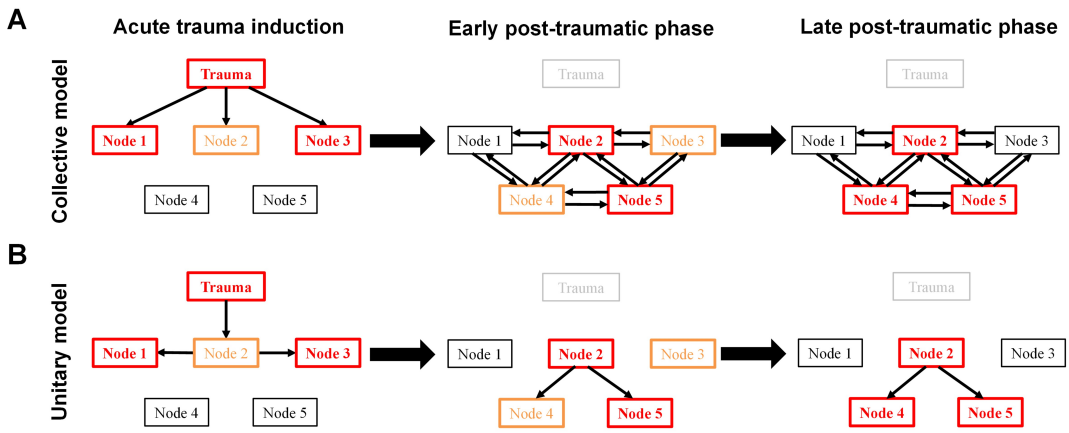

Figure 1. Two conceptual models explain the incubation process during post-traumatic stress development. Causal relations (arrows) among different psychological elements (Node #, a type of emotion or cognition) for stress development during different phases in the collective **(A)** and unitary **(B)** hypotheses. Orange and red represent medium and strong trauma-induced differences, respectively. Each psychological element can be connected to an associated neural substrate, and the trauma-induced behavioral difference to the difference between the post-traumatic and pre-traumatic neural dynamical states.

To identify the psychopathological mechanisms underlying stress incubation, it is beneficial to have an experimental assay with purely psychosocial manipulations on controlled subjective experiences and a homogeneous genetic background. Laboratory rodents proved to be a reliable model system for such a purpose. Behavioral studies revealed that laboratory rodents engage in advanced social behaviors within their cognitive capacities and share similar psychological states as humans [***Ben-AmiBartal et al.*** (***2011***, 2014); ***Burkett et al.*** (***2016***); ***Smith et al.*** (***2016***)]. Specifically, laboratory rodents have been used to study stress behavior and the pharmacology of stress [***Cryan and Holmes*** (***2005***); ***Kaouane et al.*** (***2012***); ***Calhoon and Tye*** (***2015***); ***Tovote et al.*** (***2015***)]. Also, a delay period before showing substantial stress reactions was reported in the context of rodent models simulating human PTSD [***Davis*** (***1989***); ***Pamplona et al.*** (***2011***); ***Warren et al.*** (***2013***); ***Tsuda et al.*** (***2015***); ***Sillivan et al.*** (***2017***)]. Stress reactions have been studied with a wide variety of aversive stimuli, ranging from acute physical stress [***Balogh et al.*** (***2002***); ***Philbert et al.*** (***2011***)] to a prolonged period of repeated social defeat through witnessing [***Warren et al.*** (***2013***); ***Sial et al.*** (***2016***)]. A time-dependent amplification of fear expression [***Houston et al.*** (***1999***)] has historically been proposed to explain generalized avoidance, including associative fear conditioning or non-associative fear sensitization, through stress incubation in rodents [***Pamplona et al.*** (***2011***)]. The variability of emergent phenotype following trauma was proposed to be an interaction of incubated stress and fear conditioning [***Sillivan et al.*** (***2017***)].

Here, by combining behavioral scenarios, analytic methods, and psychological hypotheses, we systematically and quantitatively studied the development of stress incubation by psychobehavioral experiments in mice. We additionally analyzed morphological changes of the brain due to stress incubation by diffusion tensor imaging (DTI). We propose that a specific internal cause and its related processes play a dominant role in stress incubation. In this unitary model (Figure 1B), a single common factor underlies the otherwise independent development of post-traumatic behaviors in mice.

Results

Emergence of long-term impacts after trauma induction

To identify post-traumatic behavioral development with minimal physical impact and peri-traumatic contribution, we developed the following assay of acute witnessing trauma (Figure 2A): Partnership between the male focal mouse and its male partner was established by housing them together for 3 weeks (Day-21–Day0). During this pair-housing, the mice slept together in a single nest which they built, and no aggressive interaction was observed. On Day0 (trauma induction), the focal mouse observed its partner being attacked by 5 different aggressor mice in succession (aggressive encounter), and stayed together with the attacked partner between each aggressive encounter (stress infiltration and resting). Importantly, the focal mouse only experienced the traumatic event by witnessing the attacks and by social communication, but not through any direct physical threat, such as attack bites and pursuits from either the aggressors or its partner. After the last aggressive encounter, the focal mouse (Partner-observing mouse) was socially isolated for 4 weeks (Day0–Day28). Behavior was tested on Days -7, 1, 7, and 28.

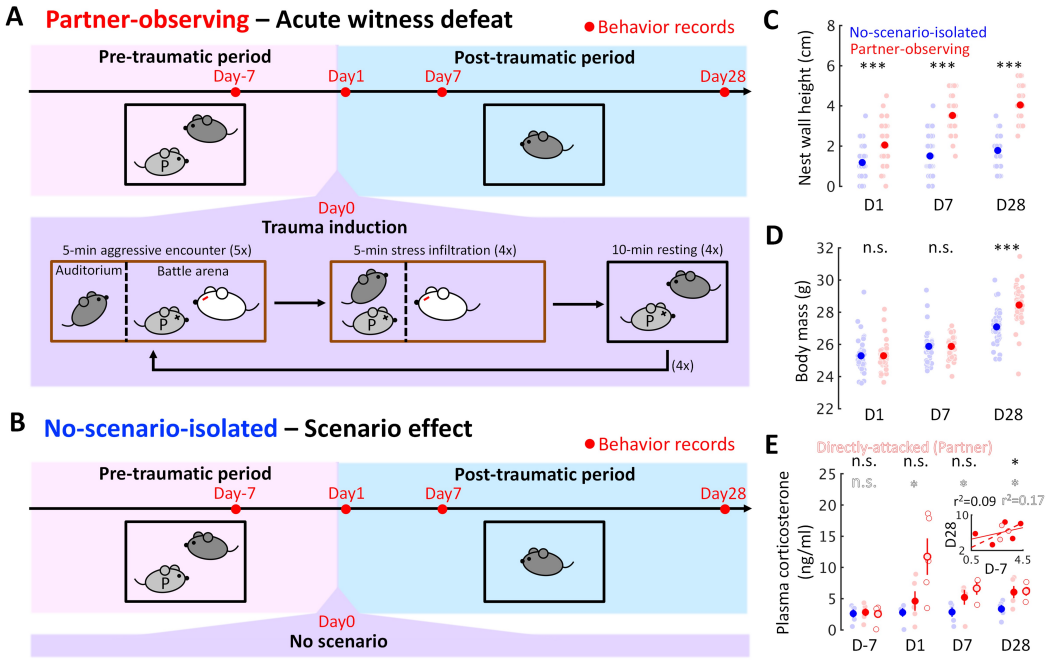

Figure 2. Acute induction of observational stress produces long-term and delayed effects on multiple behaviors and physical conditions. **(A)** Paradigm inducing acute psychosocial trauma in mice (Partner-observing mice). Focal mouse (dark gray; the Partner-observing mouse), partner mouse (light gray P), aggressor mouse (white), focal mouse's homecage (black), aggressor's homecage (brown), and wire-meshed divider (dashed line). **(B)** Experiments of No-scenario-isolated mice which had no experience of trauma induction identified the scenario effect in the behavioral paradigm. **(C)** Nest wall heights show long-lasting significant differences after trauma induction. **(D)** Body masses show significant delay difference after trauma induction. **(E)** Baseline plasma corticosterone levels show delay expression of long-lasting significant differences after trauma induction for both Partner-observing mice and their partners (Directly-attacked mice). The individual variation of this chronic impact was not predicted by the baseline plasma corticosterone levels before trauma. Light dots or lines, data of individual mice; deep dots or lines, means across populations; deep vertical lines, standard errors in the means; open circles, open words, or dashed lines, data with respect to Directly-attacked mice; n.s., $p \geq 0.05$; *, $0.01 \leq p < 0.05$; ***, $p < 0.001$;statistical significance of the difference in mean values was determined with a two-tailed, two-sample Student's t-test.

To differentiate behavioral consequences from the trauma induction and the effects of isolation, adaptation to the tests, and aging, a control group of mice were isolated from their partners on Day0 without trauma induction (No-scenario-isolated mice; Figure 2B). We found that Partner-observing

mice (n = 47) built nests with significantly higher walls than those constructed by No-scenario-isolated mice (n = 47) after isolation (Figure 2C). Partner-observing mice also increased their body masses in the late phase of the study (Figure 2D), together clearly indicating a long-term effect of trauma. While these differences could be alternatively explained (e.g. having better emotional stability and therefore nicer nests and better appetites *v.s.* manifesting protective responses of anxiety by hiding behind higher nest walls and engaging in anxiety-induced binge eating [***Goto et al.*** (***2014***); ***Otabi et al.*** (***2017***)]), we further measured a physiological indicator of observational stress, the corticosterone concentrations in blood plasma [***Ben-AmiBartal et al.*** (***2016***)]. Compared with No-scenario-isolated mice, Partner-observing mice showed higher baseline plasma corticosterone level after trauma, which reached statistical significance on Day28 (Figure 2E). To confirm the stress reactions suggested by the baseline plasma corticosterone level, in this experiment, we also isolated the attacked mice and collected their blood samples after trauma (Directly-attacked mice; n=5, note that 2 out of 5 mice died on Days 4 and 5, supposedly due to a serious depression-like anorexia as no obvious physical trauma occurred; interestingly, such losses were not observed in attacked mice which were subsequently group-housed). The tendency of higher baseline plasma corticosterone level was also observed in Directly-attacked mice which had a more obvious baseline corticosterone increment during the early phase (Figure 2E), supporting the interpretation that the observed behavioral differences might be behavioral phenotypes of stress.

An increment of corticosterone concentration is a neuroendocrine stress response [***Yehuda et al.*** (***2015***)]. Maintenance and development of the observed changes after trauma induction could be caused by a positive feedback, through an initially higher corticosterone concentration that leads to a stronger difference in the late phase. However, the baseline plasma corticosterone levels on Day-7 was poorly correlated with that on Day28 (Figure 2E, inserted panel), showing that the baseline corticosterone level before trauma induction failed to predict the individual level after trauma. This suggests that the emergence and development of post-traumatic phenotypes should be explained by a neural mechanism beyond the neuroendocrine response system.

To investigate morphological changes in the brain, we used DTI of brains collected on Day28 to analyze brain-wide microstructural differences (Figure 3): Instead of a structural change in the hypothalamus [***DeMorrow*** (***2018***)], significant differences mainly occurred in both neocortex and hippocampus. In particular, for Partner-observing mice, compared with No-scenario-isolated mice, their DTI-based fractional anisotropy (FA; Figure 3A) was lower in anterior cerebral cortical areas including the primary somatosensory cortex, anterior cingulate cortex, and orbital cortex, but higher in posterior cerebral cortical areas including the retrosplenial cortex and the primary visual cortex. It was also higher in the hippocampus. Different measures of DTI-based water diffusivities [mean diffusivity (MD), axial diffusivity (AD), and radial diffusivity (RD); Figure 3, B to D] was generally higher in the cerebral cortex and hippocampus of Partner-observing mice than in No-scenario-isolated ones. Interestingly, we observed an obvious asymmetry of the brain areas: Gray matters including the cerebral cortex and hippocampus showed differences in the right brain hemisphere, while white matters including the corpus callosum, anterior commissure, and cingulum bundle showed differences in the left brain hemisphere. The asymmetry of diffusivity between the right and left brain hemispheres were significantly enhanced in the amygdala (the right higher than the left) and areas of the lateral cerebral cortical subnetwork including dorsolateral orbital cortex and insular cortex (the left higher than the right) for Partner-observing mice. These observations support the idea that the emergence of long-term impacts after trauma induction arise from a higher-order process of cognition and emotion.

Evidence of stress development revealed by fine-scale behavioral analysis

To monitor emotionality, the observable feature demonstrated to represent emotion, of Partner-observing mice in different phases after trauma, we investigated the spontaneous behaviors of Partner-observing mice by using standard behavioral testing setups. Although the generally believed validity to identify rodent emotionality in standard behavioral tests has been criticized [***Ramos***

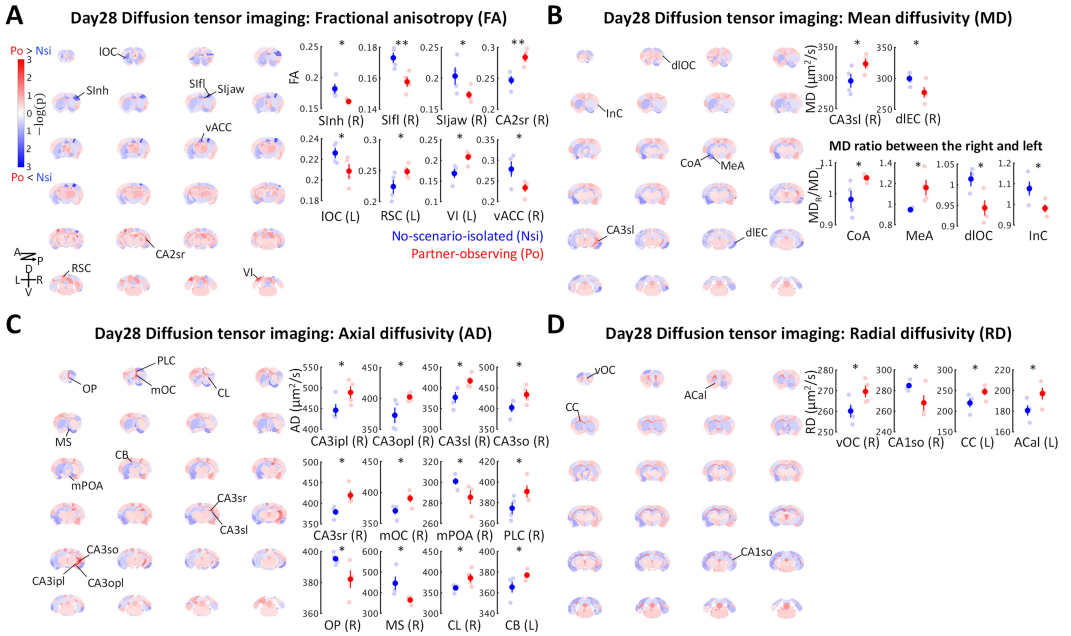

Figure 3. Diffusion tensor imaging (DTI) reveals chronic effect of acute observational stress on microstructures in the brain. **(A)** Fractional anisotropy (FA) of DTI-based water diffusivity suggests the changes of average microstructural integrity in multiple areas of the cerebral cortex. A, anterior; P, posterior; D, dorsal; V, ventral; L, left; R, right; lOC, lateral orbital cortex; SInh, non-homunculus region of the primary sensory cortex; SIfl, forelimb region of the primary sensory cortex; SIjaw, jaw region of the primary sensory cortex; vACC, ventral region of the anterior cingulate cortex; CA2sr, stratum radiatum of the hippocampal cornu ammonis (CA) 2 area; RSC, the retrosplenial cortex; VI, the primary visual cortex; (R), the right area; (L), the left area. **(B)** DTI-based mean water diffusivity (MD) suggests the changes of membrane density in multiple areas of the entorhinal cortex-hippocampus system and the straitening of structural hemispheric specializations in the amygdala-insular cortex system. dlOC, dorsolateral orbital cortex; InC, the insular cortex; CoA, the cortical amygdalar nucleus; MeA, medial amygdalar nucleus; CA3sl, stratum lucidum of the hippocampal CA3 area; dlEC, dorsolateral entorhinal cortex. **(C)** DTI-based axial water diffusivity (AD) suggests the changes of neurite organization in multiple areas of the cerebral cortex and white matter mainly in the right hemisphere. OP, olfactory peduncle; PLC, prelimbic cortex; mOC, medial orbital cortex; CL, claustrum; MS, medial septal complex; mPOA, medial preoptic area; CB, cingulum bundle; CA3sr, stratum radiatum of the hippocampal CA3 area; CA3sl, stratum lucidum of the hippocampal CA3 area;CA3so, stratum oriens of the hippocampal CA3 area; CA3ipl, inner pyramidal layer of the hippocampal CA3 area; CA3opl, outer pyramidal layer of the hippocampal CA3 area. **(D)** DTI-based radial water diffusivity (RD) suggests the changes of myelination in multiple areas of the cerebral cortex in the right hemisphere and the white matter in the left hemisphere. vOC, ventral orbital cortex; ACal, anterior limb of the anterior commissure; CC, corpus callosum; CA1so, stratum oriens of the hippocampal CA1 area. **, 0.001≤p<0.01.

(***2008***)], spontaneous behavior in a steady environment is arguably a representation of internal states such as emotion [***Archer*** (***1973***)]. In humans, anxious behaviors show when facing unexpected events or uncertain situations [***Grupe and Nitschke*** (***2013***)]. Behavioral tests for rodent anxiety-like reactions were therefore designed to evaluate their stress reaction against their willingness to explore (e.g. light-dark box and elevated plus-maze) or their activity under conditions with a gradient of uncertainty (e.g. open field). We first examined spontaneous behaviors in the light-dark box test (Figure 4A; n = 8 mice for each group), where the stressor was a natural aversion to brightly lit areas [***Kumar et al.*** (***2013***)]. Surprisingly, while the time spent in the light area did not differ significantly between No-scenario-isolated and Partner-observing mice on Day1, Partner-observing mice spent more time in the light area than No-scenario-isolated mice on Days 7 and 28 (Figure 4A, left panels). Although repeated testing effects strongly question the validated interpretation of animal behaviors in standard tests [***Lister*** (***1987***); ***Russell and Williams*** (***1973***); ***Voikar et al.*** (***2004***)], this result, as the

first glance, suggests delayed expression of a chronic behavioral difference.

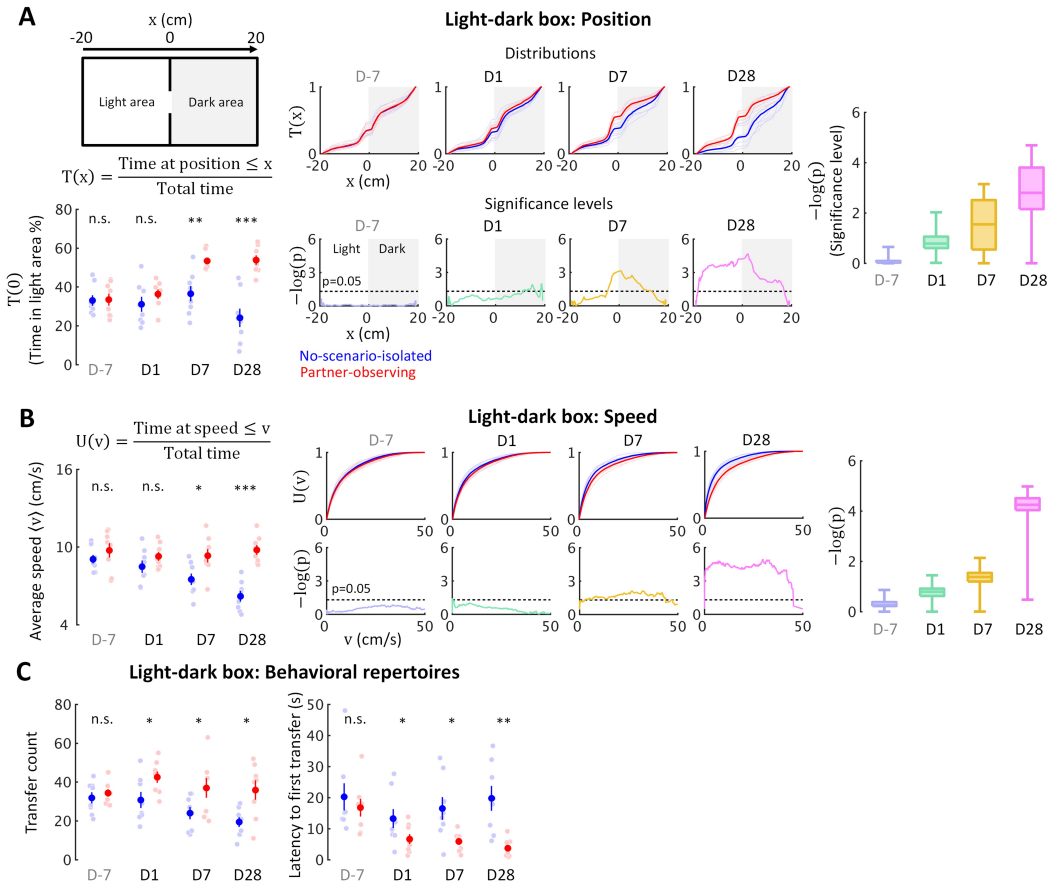

Figure 4. Fine-scale behavioral analysis in light-dark box test detects the gradually developing process of the behavioral difference. **(A)** Light-dark box test quantified through the cumulative position probability T(x) along the light-dark axis (left; total time = 300 s). On average, Partner-observing mice (red) spent more time in the light area than No-scenario-isolated mice(blue) during the late post-traumatic period [T(0), bottom-left]. Spatially fine-scale behavioral analysis reveals significant differences between Partner-observing and No-scenario-isolated populations already in the early post-traumatic period (middle). For each position, we compute the mean T(x)across the No-scenario-isolated and Partner-observing populations and compute statistical significance through a two-population Student's t-test. These differences gradually increased, as evidenced by significance distributions collapsed across all positions (right; box plots show the minima, lower quartiles, medians, upper quartiles, and maxima). **(B)** We similarly quantified speed using the fine-scale cumulative distribution U(v)of having speed ≤v and we show the statistical analysis of population differences in U(v). Cumulative distribution functions of locomotion speed (U(v) of having speed ≤v) and corresponding significance distributions provide an additional independent behavioral index that showed a gradually increasing differences of higher speed in Partner-observing mice. **(C)** Higher transfer counts and shorter latency to the first transfers in Partner-observing mice suggest their higher activity and exploratory motivation, respectively.

This result raised the following questions: (i) Did this behavioral difference start to develop immediately after the traumatic event or only after a delay? (ii) What comparative emotionality does this behavioral difference indicate?

To answer the first question (i), we examined the fine-scale positions of the mice in the light-dark box. Emotion dynamically maps internal states and external stimuli toward a set of corresponding behaviors [***Pessoa*** (***2008***)], which should be represented in the probability distribution of behaviors that are shown. Based on spatial symmetry, we analyzed T(x), the cumulative probability distribution of time that the mouse spent at positions along the axis of the light-dark box (Figure 4A, top-right

scheme and the equation, and middle panels for the results). We calculated significance levels [presented as -log of *p*-values, -log(p)] of T(x) between Partner-observing and No-scenario-isolated populations by computing position-dependent population means and applying a two-tailed, two-sample Student's *t*-test (Figure 4A, bottom-middle panels). Already on Day1, Partner-observing mice showed differences in their spatial distribution, as they spent less time than No-scenario-isolated mice at the far end of the dark area. This tendency increased with time: On Day 7, Partner-observing mice spent more time in the light area close to the door compared to No-scenario-isolated, and then on Day 28 additionally on the far side of the light area. Collapsed -log(p) distributions reveal the overall gradual increase in spatial preference differences (Figure 4A, right panel). Additionally, Partner-observing mice maintained a higher locomotor speed compared to the gradually decreasing speed of No-scenario-isolated mice (Figure 4B) and showed more transfers between the boxes and shorter latencies until their first transfers from Day 1 (Figure 4C). These results indicate an onset and gradual increase of behavioral differences immediately following the trauma.

Regarding the second question (ii), these differences may reflect the hypo-sensitivity to sensory harm and hyper-activity, such as the characteristic of somatic anxiety observed in PTSD patients [***Cloninger*** (***1988***); ***Adler et al.*** (***2004***); ***Mostoufi et al.*** (***2014***)]; however, they may also simply indicate that Partner-observing mice became braver and more excited. To determine whether the differences could be attributed to chronic anxiety, we examined their behaviors in the elevated plus-maze test (Figure 5A; n = 8 mice for each group). In this test, stressors included fear of falling and exposure, which accompanied both sensation and cognitive interpretation [***Kumar et al.*** (***2013***)]. Reactions of cognitive anxiety are expected to be opposite of those shown in somatic anxiety [***Cloninger*** (***1988***)]. After first exposure on Day-7 and separation, mice spent only a fraction of the time in the open arms of the maze, but with no significant difference between No-scenario-isolated and Partner-observing mice (Figure 5A, left panels). However, Partner-observing mice spent increasingly more time in the far end of the closed arms (Figure 5A, middle panels) and moved more slowly in the elevated plus-maze after trauma induction (Figure 5B) with longer periods of freezing and fewer entries to the central platform from the closed arms (Figure 5C). Together, this indicates a higher anxiety level and supports the hypothesis that behavioral differences are the result of a chronic anxiety. Gradually increasing differences between No-scenario-isolated and Partner-observing mice (Figure 5, A and B) further confirm that stress incubation of anxiety caused the observed differences.

Development of different psychological components untangled in standard behavioral tests

To date, the controversy at the core of stress incubation that has not been directly addressed is the source and process of internal psychological development. That is, rather than exploring determinants correlated to a developmental phenotype or asking how altered behaviors are generated by an adjusted neural controlling system [***Hayes et al.*** (***2012***); ***Calhoon and Tye*** (***2015***)], the central issue on an internal psychological development is to understand how the dynamics of internal causes intrinsically lead to specific changes of the system and resulting behaviors. Specifically, two questions should be addressed: (i) How does a trauma-induced state spontaneously affect trauma-independent states? (ii) How does increasing stress spontaneously increase? To achieve insights through further investigations, we in sequence identified different psychological components represented in mouse behaviors, demonstrated their associations in stress development, determined what cause-effect system could account for the observed processes, and validate the conceptual framework by testing its explanatory and predictive power on a wide range of control, rescuing, and physiological conditions.

A prolonged fear sensitization was hypothesized to induce a generalized, trauma-independent avoidance [***Pamplona et al.*** (***2011***)]. To explore the developmental process of different psychological components, we first investigated the emotional representations further revealed in fine-scale behavioral distributions. In both tests, key incubation features were consistently more obvious

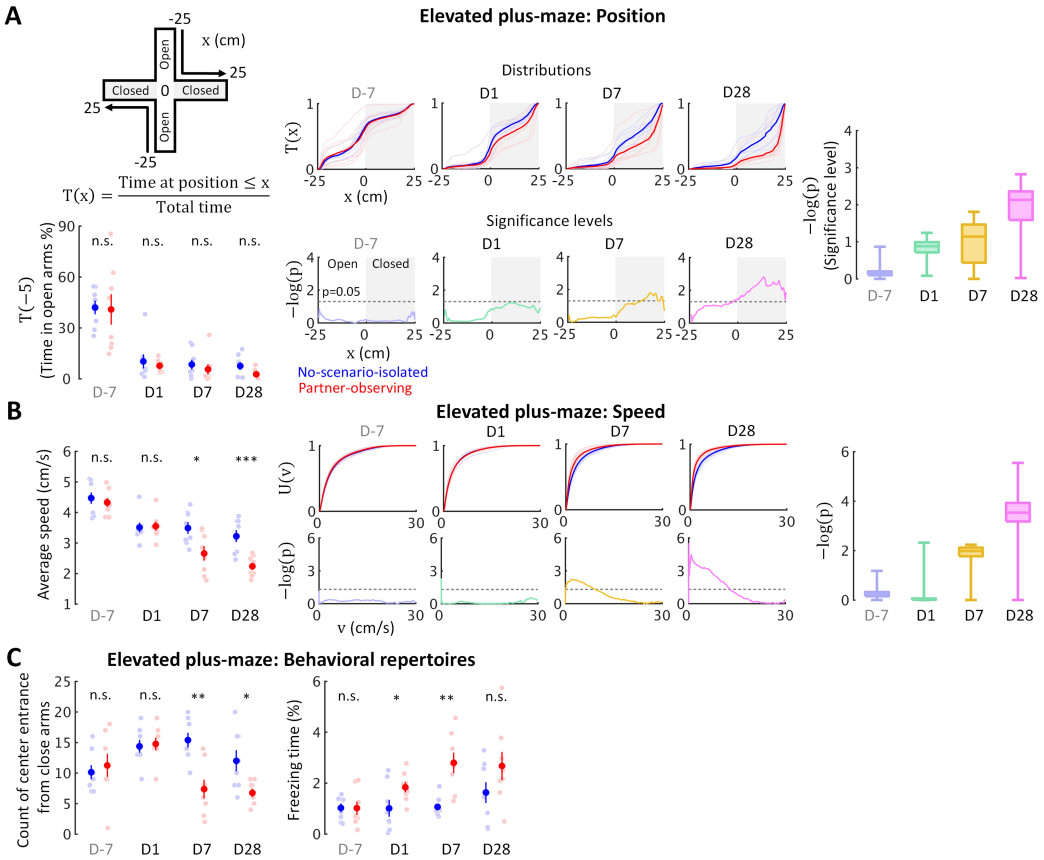

Figure 5. Behavioral testing in the elevated plus-maze demonstrates that stress incubation of anxiety caused the observed differences. **(A)** Partner-observing and No-scenario-isolated mice did not differ significantly in the time they spent in opened arms (total time = 300 s); however, spatial distributions show differences in preferred location between Partner-observing and No-scenario-isolated mice in the closed arms, which increased with time. **(B)** Cumulative distribution functions of locomotion speed and corresponding significance distributions show a gradually increasing differences of lower speeds in Partner-observing mice. **(C)** Less exploration from close arms to platform center and longer freezing time in Partner-observing mice suggest their stronger stress reactions.

within stressor-free zones (dark area and closed arms) than within stressor zones (light area and open arms), and thus the features of the behavioral response might change depending upon whether mice were under the stressor. To quantitatively investigate the differences between zones, we analyzed locomotor speed, as an independent behavioral index of mouse position, separately in stressor and stressor-free zones (Figure 6). As expected, two different behavioral patterns developed in the two zones: While speed differences consistently increased in stressor-free zones (Figure 6, B and D), speed differences in stressor zones only showed acute increases on Day1 (Figure 6, A and C). These results suggest that different psychological features were measured in the two zones, allowing further identification of association among different trauma-induced states.

Following the observation, we next asked what psychological basis could account for the two behavioral features separately measured in the stressor and stressor-free zones. In humans, fear is a response to a known threat with a magnitude that increases with the certainty of the threat, whereas anxiety is a response to uncertainty with a magnitude that increases with the uncertainty of a situation [***Grupe and Nitschke*** (***2013***)]. Together with the presented demonstration of anxiety incubation (Figures 4 and 5), we hypothesized that behavioral differences in stressor-free zones are the result of anxiety reactions to uncertainty, while acute stress reactions in stressor zones are the result of lasting fear responses from trauma induction. We examined mouse locomotor

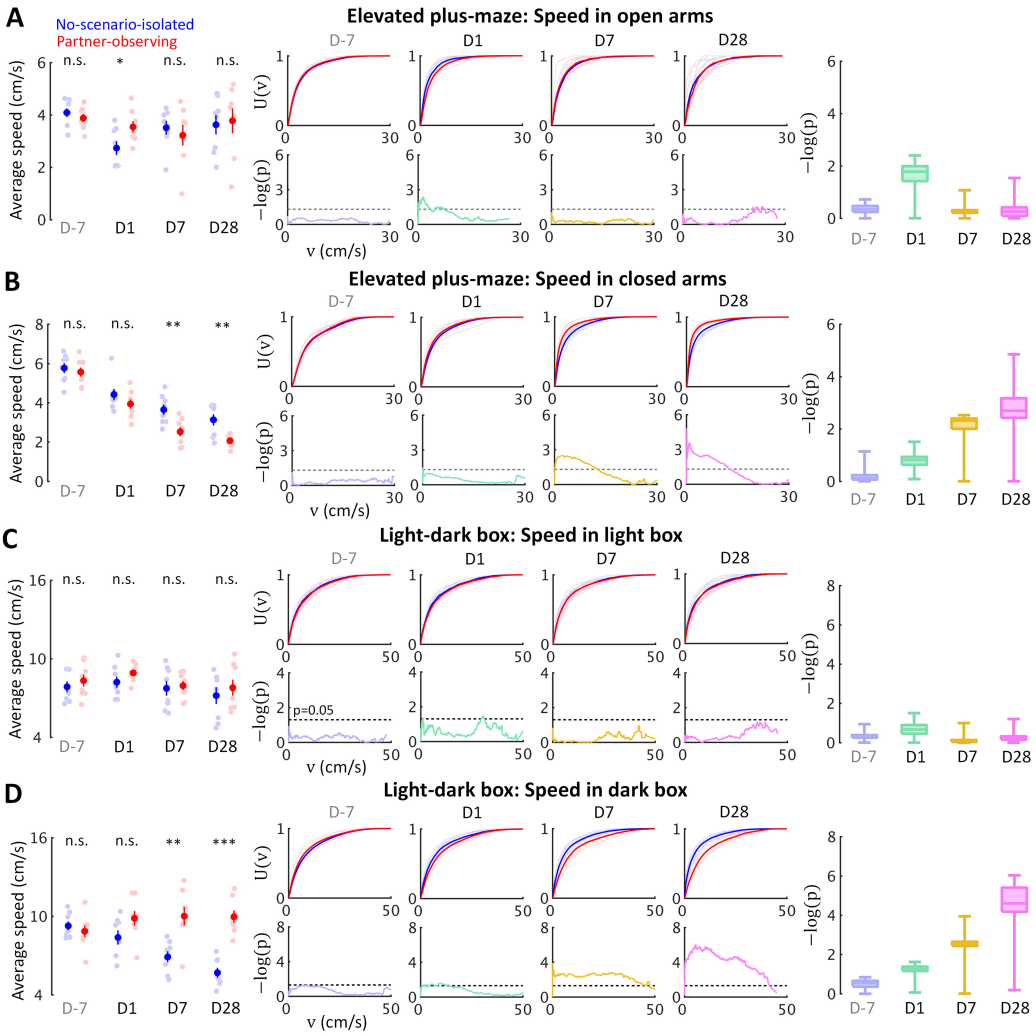

Figure 6. Gradually increasing anxiety and acute fear reaction were untangled in standard behavioral tests as different psychological components with distinctive developments. Locomotion speed shows acute difference only in stressor zones [open arms **(A)** and light area **(C)**], but incubated differences in stressor-free zones [dark area **(B)** and closed arms **(D)**].

speed in uncertain and familiar environments separately using the open field test (Figure 7, A to C; n = 8 mice for each group) and the locomotor activity test (Figure 7D; n = 8 mice for each group), respectively. In the open field test, mice were exposed in a dimly lit environment with a gradient of spatial uncertainty from the field center (high uncertainty) to field boundaries (low uncertainty). In the locomotor activity test, mice were habituated in a dark environment with familiar cues of bedding materials from their homecages indicative of less environmental stress. Compared to No-scenario-isolated mice, Partner-observing mice moved faster in the center region of the open field (Figure 7A), which was not observed in the periphery (Figure 7B). The difference between groups increased gradually in the center but not in the periphery (Figure 7, A and B). The avoidance of spatial uncertainty by Partner-observing mice was also reflected in the shorter time they spent near the center (Figure 7C, left panel) and showed a shorter latency to the first rearing during the test (Figure 7C, right panel), which together suggests anxiety, represented in a high tension between high uncertainty avoidance and high exploratory motivation, as the causal emotional state. In contrast, Partner-observing mice moved significantly more slowly on Day1 in the locomotor activity test, and recovered on Days 7 and 28 (Figure 7D), suggesting that the post-tramatic impact

was acute when mice reacted to a switched condition with high certainty and less stress. These results support the hypothesized psychological basis of anxiety and fear that account for the two behavioral features with separated developments.

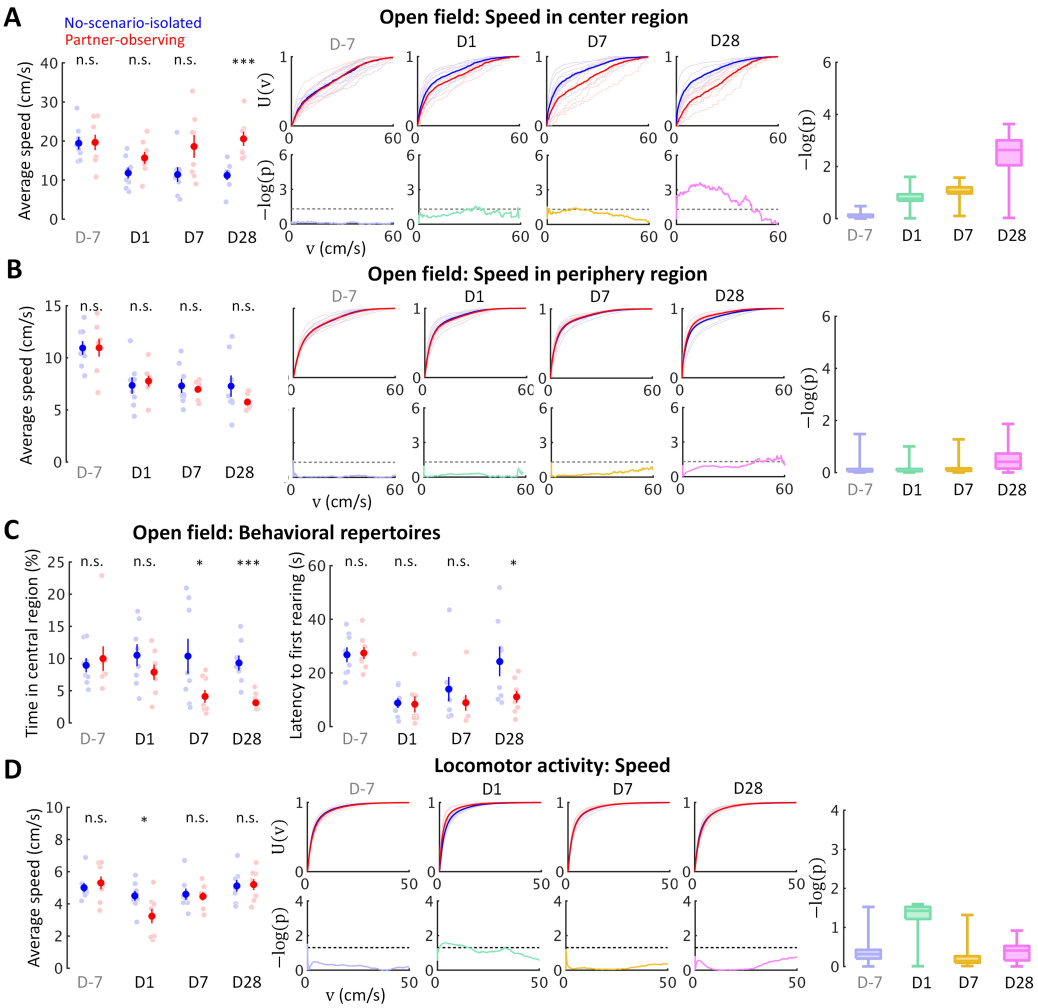

Figure 7. Behavioral testing in the open field test and locomotor activity test confirms distinctive psychological substrates and their corresponding development patterns. **(A)** Anxiety is evident in the open field test through a delayed onset of locomotor speed differences in the center region with higher spatial uncertainty. **(B)** The differences of locomotor speed observed in the center region did not occur in the periphery region with lower spatial uncertainty. **(C)** Less time spent in the central region by Partner-observing mice suggests their avoidance of a region with high special uncertainty, while shorter latency to their first rearing indicates their higher exploratory motivation. **(D)** In the locomotor activity test without stressors, acute effects of activity reduction recovered in the later post-traumatic period.

Notably, these observations of mouse spontaneous behaviors in the light-dark box test, elevated plus-maze test, open filed test, and locomotor activity test (Figures 6 and 7) indicated a previously unexpected association between different post-traumatic stress reactions: These results revealed that the two developmental patterns displayed a consistent uncertainty-dependent manner which was validated across multiple behavioral tests. In addition, the patterns raised together in the acute phase, but one vanished when the other continued to increase in the later phase. These results imply that delayed anxiety expression is hard to simply be considered as an expanded, sustained response of fear memory or a stress reaction of which the emergence is induced by fear memory, thereby refuting a general belief [***DSM-III*** (***1980***); ***DSM-5*** (***2013***); ***Ehlers and Clark*** (***2000***); ***Siegmund***

and Wotjak (***2006***); ***Andrews et al.*** (***2007***); ***Pamplona et al.*** (***2011***); ***Hayes et al.*** (***2012***); ***Zoladz and Diamond*** (***2013***); ***Schnyder and Cloitre*** (***2015***); ***Bryant et al.*** (***2017***)].

Comparison of emotionality and sociality differences proffers a unitary model

Although we have demonstrated that the incubated anxiety and acute non-associative fear memory could be independent in our paradigm, this indication does not distinguish a unitary model from a collective model (Figure 1A): In a unitary model, the incubated anxiety and acute non-associative fear memory are independently mediated by the trauma-induced state of a common psychological component, and the incubated anxiety does not induce generalized behavioral changes in the late phase. In a collective model, incubated anxiety and acute non-associative fear memory can be independently and directly induced by the traumatic event, while the incubated anxiety can also further induce generalized behavioral changes in the late phase. To test both model against each other, we study the relation between emotionality, specifically anxiety, and sociality in our paradigm.

Emotional responses simplify and speed up animal reactions to complex external cues and are critical in corresponding social interactions [***Anderson*** (***2016***)]. If a sociality difference occurs and it is induced by incubated anxiety, as in the case of the collective model, the growing pattern of incubated anxiety should temporally precede or co-emerge with the corresponding growth pattern of sociality difference. Additionally, the sociality difference should be anxiety-correlated, and therefore should not occur without incubated anxiety. In the alternative unitary model, if the sociality difference develops independently after trauma induction and is independent of the incubated anxiety, then the sociality difference can preceed the incubated anxiety and should be independent of incubated anxiety.

To test potential effects of anxiety on sociality, we examined mouse social motivation in a two-session social test (Figure 8A): A non-social session followed by a social session (n = 5 mice for each group). The social stimulus was either a female or a male stranger mouse.

During the social session, Partner-observing mice spent less time in social approaches of nose poking toward both female and male strangers, starting from Day1, and remained less social compared to No-scenario-isolated mice during the post-traumatic period (Figure 8B). The time they spent in the interaction zone around the social target, however, did not differ significantly from that of No-scenario-isolated mice (Figure 8C). Both, Partner-observing and No-scenario-isolated mice, spent only a short but similar time on nose poking during the non-social session through the recordings on different days, with no significant difference between Partner-observing and No-scenario-isolated populations (Figure 8D), indicating that the observed difference of nose poking time was socially specific. In addition, less social vocalization was recorded during the female stranger test for Partner-observing mice (Figure 8E). These results indicated a general and chronic reduction of social interest developing after the trauma (Figure 8-video supplement 1). This reduction of social interest differs from social avoidance due to anxiety because the social target is not avoided but just ignored [***Sial et al.*** (***2016***); ***Krishnan et al.*** (***2007***)].

We also analyzed locomotor speed of mice in empty sessions as an indicator of emotionality previous to social sessions, and find a notable drop of spontaneous locomotor speed starting on Days 7 and 28 (Figure 8F). Interestingly, onset of chronic reduction of social interest (starting from Day1) preceded the drop of locomotor speed. These results suggest that the changes of emotionality and sociality arise independently after trauma induction.

Relationship-dependent behaviors suggesting affectional mechanism

Two possibilities remain that could still explain a collective model: The sociality difference could be a higher-order consequence of incubated anxiety (Figures 4, 5, 6 and 7) or it could also be a parallel mechanism induced directly by the traumatic event. However, the following experiments reject these possibilities (Figure 9):

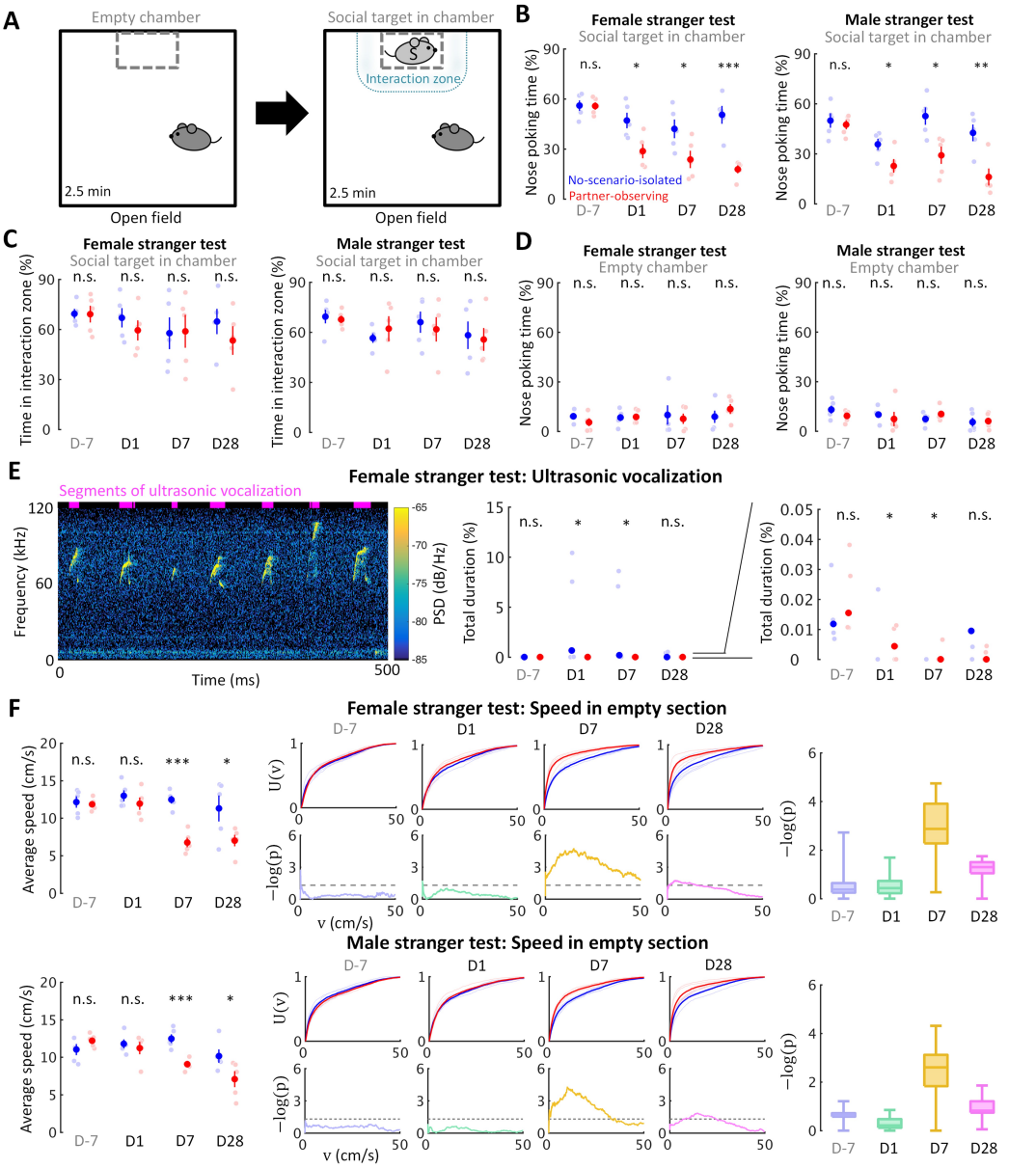

Figure 8. Acute psychosocial trauma decreases social interest. **(A)** The active social interaction test with consecutive non-social and social phases. During the social phase, motivation for social contact toward a stranger mouse (light gray S) was evaluated as the time spent for social approaches of nose poking and the time spent in the delineated interaction zone. **(B)** Partner-observing mice made fewer nose poking to both female (left) and male (right) strangers. **(C)** There was no significant difference in the time spent in the interaction zone during the social phase, suggesting a decrease of social interest instead of an active social avoidance. **(D)** There was no significant difference in the time spent of nose poking during the non-social phase, confirming that the observed differences of nose poking time stemmed from a specifically social root. **(E)** Spectrogram of short but conspicuous ultrasonic vocalizations emphasizes a specific behavioral repertoire during the social session in the female stranger test of a No-scenario-isolated mouse on Day1. More vocalization was recorded from No-scenario-isolated mice than Partner-observing mice on Days 1 and 7. Reduced ultrasonic vocalization during the social session of the female stranger test in Partner-observing mice attests to diminished social communication. Note that data points greater than 0.05% are not visible in the right panel which zoom in the data of the middle panel to emphasize the data distributions in the range of 0–0.05%. Data points and median, one-tailed Mann-Whitney U test; PSD, power spectral density. **(F)** Partner-observing mice showed a delayed onset of reduction in locomotion speed during the non-social phase. The following video supplement is available for figure 7: video supplement 1.

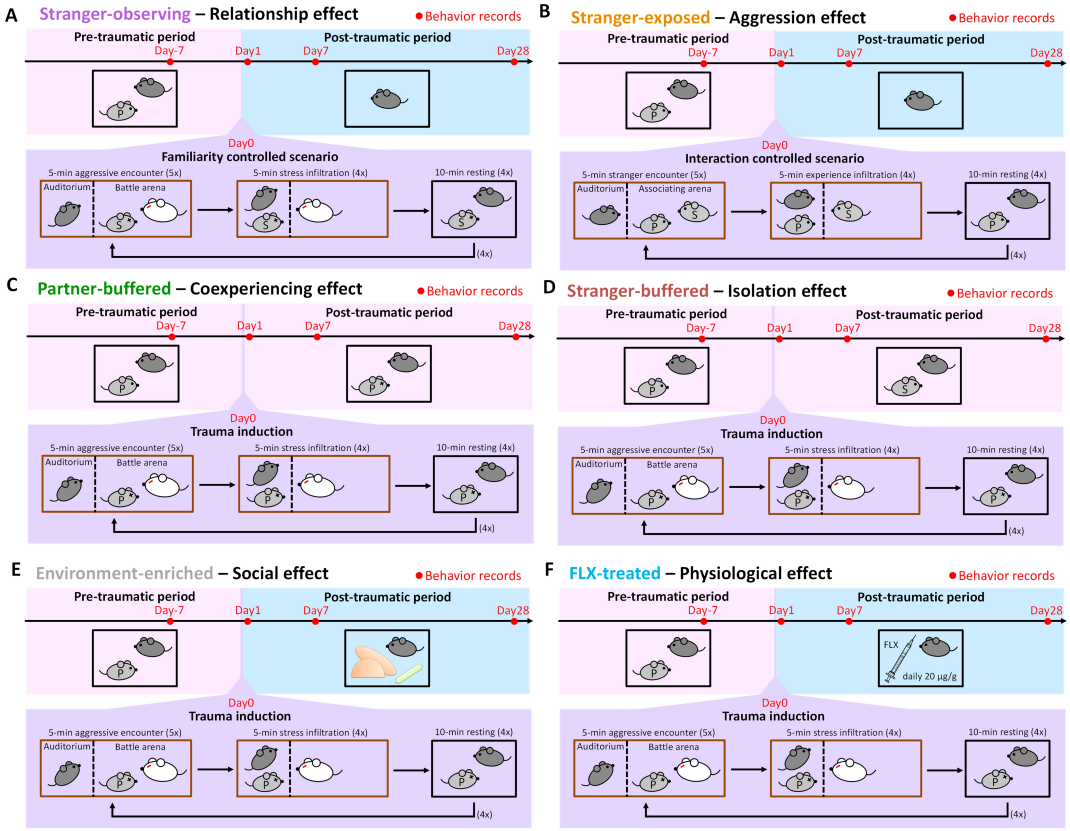

Figure 9. Control experiments investigate psychosocial and physiological factors that determined and recued the behavioral developments. **(A)** Experiments of Stranger-observing mice which had witnessing experience of trauma that happened to strangers, rather than to their pair-housed partners, identified the relationship effect in the behavioral paradigm. **(B)** Experiments of Stranger-exposed mice which had experience of social interactions without witnessing stress from strangers identified the aggression effect in the behavioral paradigm. **(C)** Experiments of Partner-buffered mice which were pair-housed with their partners after trauma induction identified the social transfer effect of coexperiencing trauma in the behavioral paradigm. **(D)** Experiments of Stranger-buffered mice which were pair-housed with strangers after trauma induction identified the isolation effect in the behavioral paradigm. **(E)** Experiments of Environment-enriched mice which were provided with toys after trauma induction identified the social rescue effect in the behavioral paradigm. **(F)** Experiments of FLX-treated mice which were treated with fluoxetine after trauma induction identified the pharmacological rescue effect in the behavioral paradigm.

First, we show that affectional bonding is the key trauma-associated psychological factor that commonly mediated the development of both emotionality and sociality (Figure 10):

As Partner-observing mice experienced the traumatic event purely psychosocially, partnership between mice served as a candidate variable with which to alter the emotional impact and coping strategy [***Sandi and Haller*** (***2015***); ***Yang et al.*** (***2017***); ***Ben-AmiBartal et al.*** (***2014***)]. Thus, we analyzed a second group of mice (Stranger-observing mice; Figure 9A) as each of them observed different stranger mice being attacked by different aggressors and stayed together with each stranger between aggressive encounters before isolation.

Stranger-observing mice did not experience any physical stress from strangers or aggressors. Two notable behavioral differences during trauma induction were observed: While tail rattling during aggressive encounters and hiding under bedding material with the partner during resting were observed in 83% (n = 39 out of 47 mice) and 100% (n = 47 out of 47 mice) Partner-observing mice (Figure 10-video supplement 1), respectively, no such behaviors were shown by Stranger-observing mice (n = 0 out of 20 mice; n = 0 out of 20 mice). In Partner-observing mice, the frequency of tail rattles dropped progressively during aggressive encounters (Figure 10A), suggesting that it

represents a rapid phasic psychological reaction during trauma induction. These results suggest that social relationship rapidly modulated emotional impact and social reactions during trauma induction. Moreover, chronic behavioral differences were not observed in Stranger-observing mice (Figure 10, B to F), which further excluded potential effects from salient, non-specific environmental manipulation (e.g. rotation through aggressors' homecages) and sensory shock (e.g. olfactory cues from urine and vocalization indicating fear) in trauma induction. Taken together, the results reveal that social relationship constitutes a critical common psychological factor that determined post-traumatic psychobehavioral development.

Considering a unitary model with social relationship as the key factor, an important question remained: Why is stress incubated, but not attenuated? As traumatic consequences were modulated by social relationship, we hypothesized that the traumatic event resulted in gradually increasing separation distress through partnership memory during social isolation. This is analog to human patients tending to recall relatively vivid memories of the past relationship after a traumatic relationship dissolution [***Chung et al.*** (***2003***)]. Social isolation generally disrupts mouse capacities for social recognition and social memory measured in curiosity-based behavioral tests [***Kogan et al.*** (***2000***); ***Okuyama et al.*** (***2016***)]. We examined the persistence of social memory in a partner-revisiting test on Day28 (Figure 10G; n = 5 mice for each group). Social stimuli were the previous partner and a stranger mouse, both immobilized to allow enough social cues to be attractive, but no active interaction with the focal mouse. To avoid possible influences of social cues from socially defeated mice, stranger mice used to test No-scenario-isolated and Stranger-observing mice were partners of Partner-observing mice. Strikingly, Partner-observing mice spent three times as much time allogrooming or pushing their previous partners as did No-scenario-isolated and Stranger-observing mice (Figure 10, H and video supplement 2), which was opposite to the lower contacts with familiar social targets in a three-chamber social novelty test where curiosity to novelty dominates the behavior [***Okuyama et al.*** (***2016***)]. The preference of Partner-observing mice to their previous partners, together with the findings of chronic anxiety (Figures 4 and 5) and reduction of social interest (Figure 8) after separation, suggests affectional bonding as a key mechanism of stress incubation in this paradigm.

Rescue of stress development by social buffering

Next, we observed the development of sociality differences without the development of emotionality differences when testing the necessary and sufficient conditions in our paradigm (Figure 11):

Two important conditions in our behavioral paradigm were the increased number of mice during trauma induction (visual exposure to 5 different aggressors) and the forced social isolation after trauma, of which the potential effects should further be identified. We first compared behavioral developments of No-scenario-isolated mice with a third control group of mice (Stranger-exposed mice; Figure 9B) where the aggressor mice for trauma induction were replaced by non-aggressive strangers. As the expectation (Figure 10), Stranger-exposed mice did not show the developments of behavioral difference (Figure 11), confirming that social aggression is necessary to induce stress developments.

Conceptualization of social support as a "stress buffer" have been proposed to explain the positive association between responsive social resources in a small social network and adverse effects of stressful events [***Cohen and Wills*** (***1985***)]. To further characterize social effects in post-traumatic period, we examined the impact of social support on behavioral developments by a fourth control group of mice (Partner-buffered mice; Figure 9C) as each of them was kept pair-housed with its attacked partner after trauma induction. Noteworthily, developments of the differences in emotionality of stress did not occur in Partner-buffered mice (Figure 9, A to C), but importantly, developments that reflected their sociality showed the differences of Partner-observing mice (Figure 9, D and E). This observation manifested the sufficiency of socially isolated condition for anxiety incubation but not for the reduction of sociality differences. Their similarity with Partner-observing mice in a longer time spent with partners extrapolates that the partner revisiting test is

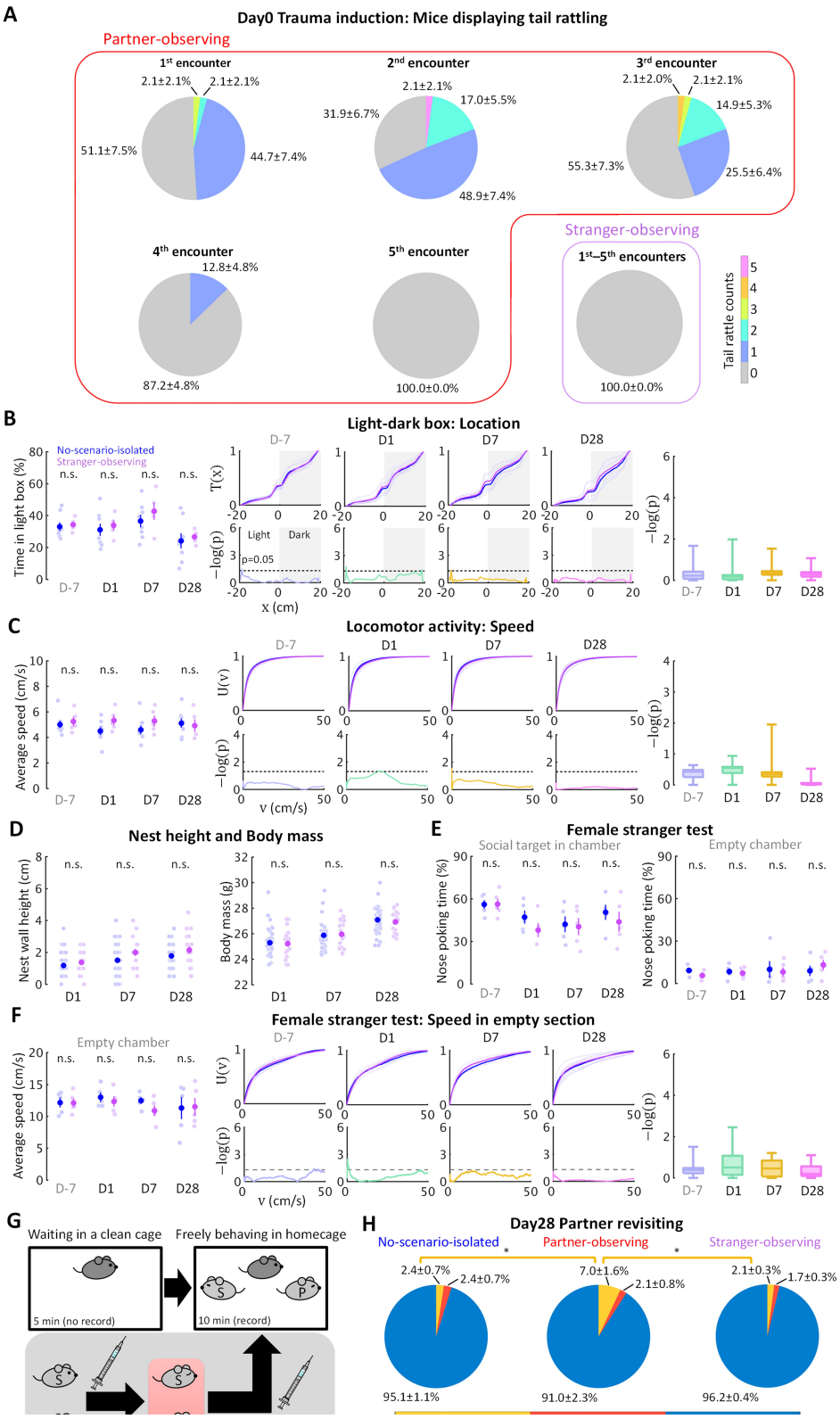

Figure 10. Social relationship in trauma induction determines stress development. **(A)** Social relationship increased emotional impact, evidenced by tail rattling behavior during trauma induction. **(B–F)** No significant chronic difference was found in Stranger-observing mice. **(G)** The partner-revisiting test. A stranger mouse (light gray S) and the previously pair-housed partner (light gray P), both immobilized, were presented as social targets. Pink rectangle, heating pad. **(H)** Partner-observing mice showed significantly longer allogrooming or pushing their partners (yellow, % of time spent in partner concern behavior) than either No-scenario-isolated or Stranger-observing mice. Standard errors were calculated from bootstrapped data. The following video supplements are available for figure 9: video supplements 1 and 2.

a memory-based assay to measure social bonding in mice. The observation also strengthens the position that emotionality and sociality during stress incubation were separately regulated.

Since Partner-buffered mice experienced the same traumatic scenario as Partner-observing mice, questions remain regarding the psychological mechanism for the partial rescue of stress development in Partner-buffered mice. Because stress reduction through social buffering depends on both social contact and social communication which can be altered by emotional contagion based on different social experiences [***Ben-AmiBartal et al.*** (***2014***); ***Burkett et al.*** (***2016***); ***Smith et al.*** (***2016***); ***Yu et al.*** (***2017***); ***Ishiyama and Brecht*** (***2016***); ***Yang et al.*** (***2017***)], and the stress-buffering resources of Partner-buffered mice experienced direct trauma, we hypothesized that, in social buffering, the development of emotionality difference is regulated by the social availability, while the development of sociality difference is regulated by the social context. To address these issues, we conducted a fifth control group of mice where each of them was kept pair-housed with a stranger after trauma induction (Stranger-buffered mice; Figure 9D), and a sixth control group of mice where each of them was provided with toys during social isolation after trauma induction (Enviroment-enriched mice; Figure 9E).

In the Stranger-buffered paradigm, we found aggressive attacks toward defeated strangers by all focal mice (n=5 out of 5) during pair-housing after trauma. Similar behavior was observed when Partner-observing mice, but not their defeated partners, were group-housed after trauma induction (non-recorded observation). While the observations importantly illustrate partnership-specific agressive behavior, we tested the behaviors of Stranger-buffered mice only for those which were pair-housed with a non-defeated stranger. For these Stranger-buffered mice, they did not displayed the developments of both emotionality and socility differences (Figure 12), with only an acute effect of positions in the light-dark box test (Figure 12A).

Notably, although Enviroment-enriched mice showed similar nose poking times in the female stranger test (Figure 12B) suggesting a rescue of sociality difference, they showed the behavioral differences of Partner-observing mice in the light-dark box test and the non-social session of female stranger test, which even had a stronger difference during the early phase (Figure 12, A and C). The data corroborate the hypothesized mechanism of social buffering in rescuing stress incubation and additionally emphasize the differential effects between social and physical environmental enrichment.

Changes in brain connectome suggest neural substrate of unitary model

Based on our behavioral results, as well as analyses of physiological consitions (Figure 2E and Figure 3), we next asked if a corresponding neural framework could account for the unitary model deduced from our psychobehavioral experiments. The major neuromodulatory system of serotonin has long been linked to broad neural controls of physiological, sensorimotor, emotional, motivational, cognitive, and social modulations [***Li et al.*** (***2016***)]. Fluoxetine, as a selective serotonin reuptake inhibitor, is widely used in prevalent disorders, including PTSD, regarding its supposed importance on inconclusive physiological roles [***Fischer and Ullsperger*** (***2017***)]. We investigated a seventh control group of mice (FLX-treated mice; Figure 9F) as each of them was injected with fluoxetine daily after trauma. Although FLX-treated mice showed less behavioral difference in the early post-traumatic phase (Figure 12, A and D) and did not display a reduction of social interest (Figure 12B), incubated anxiety kept developing and reached significance in the late phase (Figure 12, A and D). These results exposed the limitation of a global pharmacological treatment for stress incubation.

To further explore the physiological basis, beyond the DTI-based microstructures of the brain, we investigated long-range connections of the hippocampus, as the region showing the most notable differences from various measures (Figure 3). Compared with No-scenario-isolated mice, among all brain regions, DTI-based fiber tracking highlighted the significant increases of structural connections between the right hippocampus (CA3 and dentate gyrus) and right dorsolateral entorhinal cortex (Figure 13A), an area also showed difference of its mean diffusivity (Figure 3A) in Partner-observing

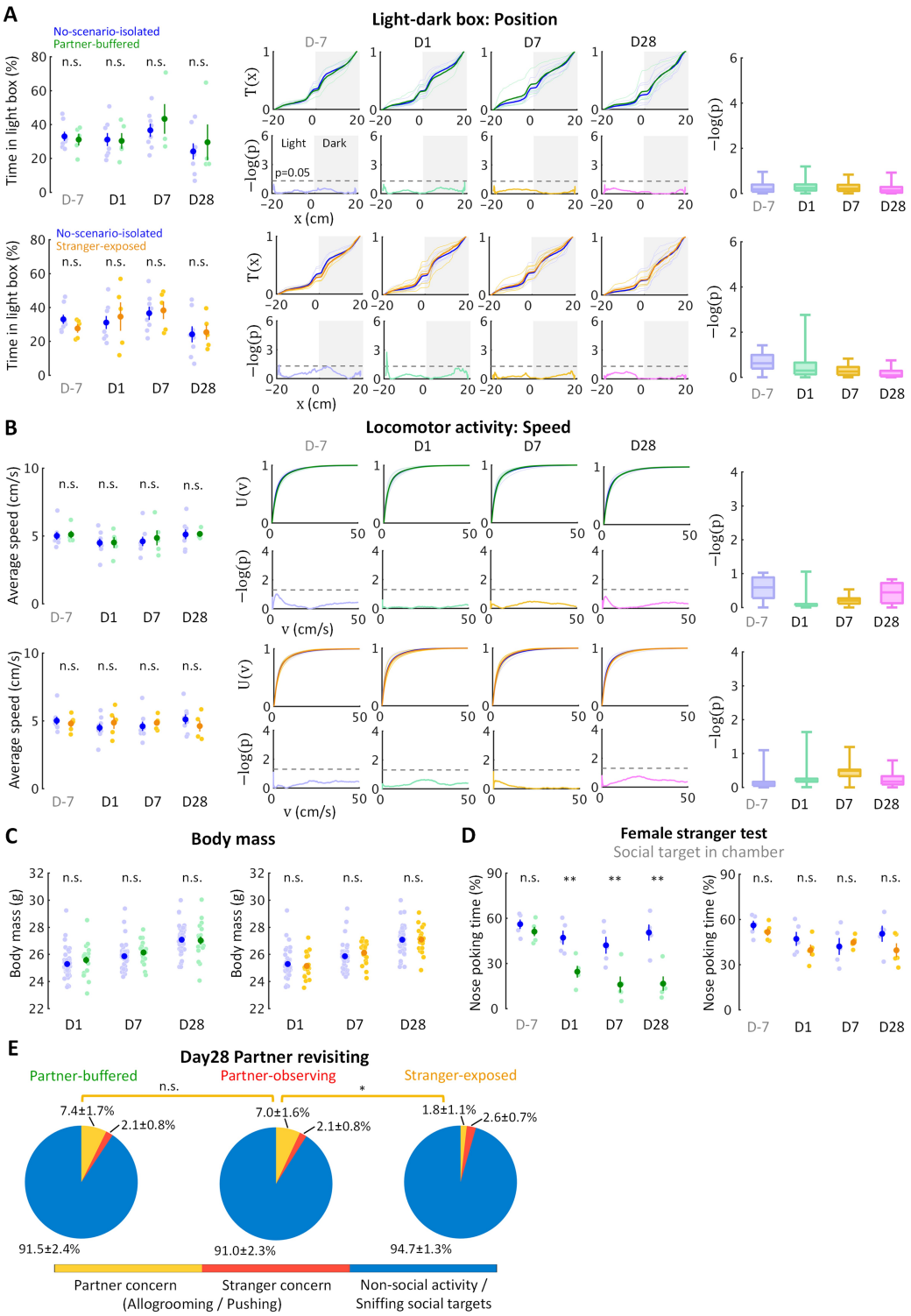

Figure 11. Control experiments identify necessity of relationship-dependent vicarious defeat and sufficiency of social isolation for anxiety incubation. **(A)** Positions in the light-dark box test indicate that Partner-buffered and Stranger-exposed mice did not develop the chronic stress reactions. **(B)** Locomotor speeds indicate that Partner-buffered and Stranger-exposed mice did not develop the acute stress reactions. **(C)** Body masses indicate that Partner-buffered and Stranger-exposed mice did not develop the physiological differences. **(D)** Nose poking times in the female stranger test indicate that Partner-buffered mice did, but Stranger-exposed mice did not develop the social differences. **(E)** Partner-buffered mice and Partner-observing mice spent longer time on the behaviors reflecting partner concern.

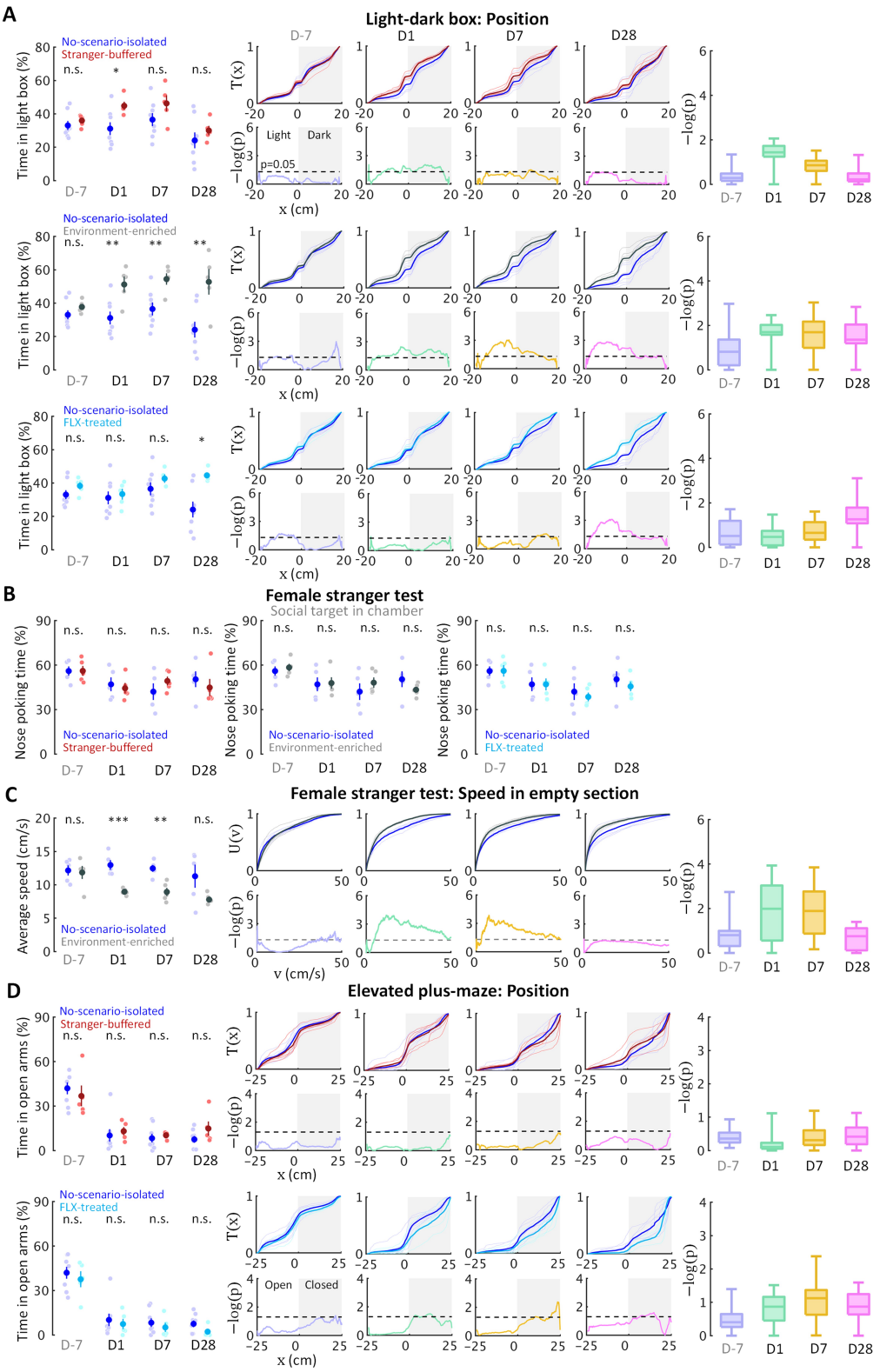

Figure 12. Control experiments uncover that social buffering with non-defeated strangers rescued the full phenotypic dimensions of stress development. **(A)** Positions in the light-dark box test indicate that Environment-enriched and FLX-treated mice did, but Stranger-buffered mice did not develop the behavioral differences in the late phase. **(B)** Nose poking times in the female stranger test indicate that Stranger-buffered, Environment-enriched, and FLX-treated mice did not develop the social differences. **(C)** Environment-enriched mice showed of reduction in locomotion speed during the non-social phase. **(D)** Positions in the elevated plus-maze test indicate that Stranger-buffered mice were better rescued than FLX-treated mice.

mice. While the entorhinal cortex is the main interface between the hippocampus and neocortex, we further tracked its long-range connections. The right dorsolateral entorhinal cortex showed significantly increased connections with the right perirhinal cortex, but had significantly decreased connections with the right piriform cortex (Figure 13A). Interestingly, the piriform and perirhinal cortices are the two core parahippocampal structures involve in the kindling phenomenon, the daily progressive increase in response severity of both electrographic and behavioral seizure activity [***McIntyre and Kelly*** (***2000***); ***McIntyre*** (***2005***)] supposedly linked to fear conditioning in rat PTSD models [***Rau et al.*** (***2005***); ***Knox et al.*** (***2012***)]. We found a decrease of the connections between the piriform and perirhinal cortices (Figure 13A). Trough further tracking, we exposed a trauma-induced changes of DTI-based connectivity framework: the perirhinal cortex-entorhinal cortex-hippocampus, retrosplenial cortex-hippocampus, piriform cortex-amyglala, and amyglala-hypothalamus systems were centered at the anterior cingulate cortex (ACC; Figure 13B), in agreement with a unitary model. These results emphasize the importance of a treatment on the specific clinical target in the full mechanistic picture according to a unitary model that explains, integrates, and predicts multiple mechanisms underlying highly diverse behavioral consequences.

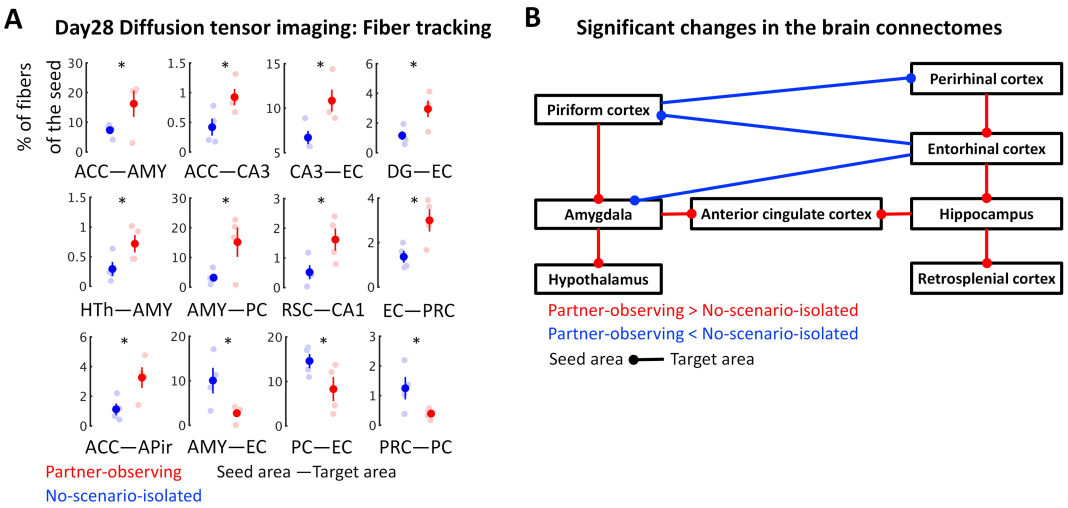

Figure 13. DTI-based long-range connections suggest neural substrate of unitary view for stress development. **(A)** DTI-based network-wise fiber tracking reveals specific chronic changes of structural connectivity in the brain. AMY, the amygdala; HTh, the hypothalamus; DG, the hippocampal dentate gyrus; PC, the piriform cortex; PRC, the perirhinal cortex; APir, the amygdalopiriform transition area. Note that the brain regions were in the right brain hemisphere. **(B)** Trauma-induced structural changes of the underlying brain connectome uncovered an enhancement of a unitary network centered at the anterior cingulate cortex.

Discussion

We present a novel approach to interpret previously challenging and inconclusive behavioral development and use it to study the internal psychological development of stress incubation in laboratory mice. These results demonstrate the first system-level view of experimentally disentangled components, processes, and determinants in post-traumatic stress development. While our data suggest that laboratory mice developed diverse post-traumatic reactions with comparable psychological features as observed in human, we found little support for the collective model view that a complex association among trauma-induced psychological states govern the developmental process [***DSM-III*** (***1980***); ***DSM-5*** (***2013***); ***Ehlers and Clark*** (***2000***); ***Siegmund and Wotjak*** (***2006***); ***Andrews et al.*** (***2007***); ***Pamplona et al.*** (***2011***); ***Hayes et al.*** (***2012***); ***Zoladz and Diamond*** (***2013***); ***Schnyder and Cloitre*** (***2015***); ***Bryant et al.*** (***2017***)] (Figure 14A). Instead, we propose a unitary model where the alteration of a single cognitive source is sufficient for triggering changes of diverse and

otherwise independent psychological states (Figure 14B). Indeed, we found that the strengthening of an ACC-centered network supports the proposed unitary model for the diversity of behavioral phenotypes.

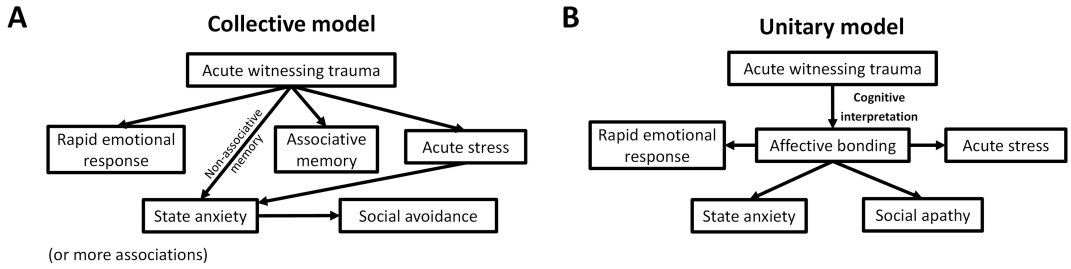

Figure 14. Foregoing data demonstrate a unitary psychopathological model with its corresponding neural substrate for the stress development paradigm in this study. Our data show little support for a collective view speculated in previous hypotheses **(A)**, but support a unitary view **(B)** where diverse PTSD-like reactions independently developed via a common cognitive source ("Affective bonding"). This unitary view suggests a psychological substrate in system-level that integrates multiple mechanisms underlying highly diverse behavioral consequences, as a specific clinical target in the full mechanistic picture.

Here we summarize our results and interpretations:

- *Did mice display stress reactions after observing a traumatic event inflicted upon their pair-housed partners?* Yes. Higher nest wall (Figure 2C), higher baseline corticosterone levels (Figure 2E), more time spent in the further end of close arms (Figure 5A), less exploration from close arms to center (Figure 5C, left panel), longer freezing time (Figure 5C, right panel), and slower locomotion (Figure 5B) in the elevated plus-maze test, more time spent in the center region (Figure 7C, left panel), and shorter latency to the first rearing (Figure 7C, right panel) in the open field test, and slower locomotion in the locomotor activity test (Figure 7D) are all classically interpreted as stress reactions. However, we also note that increased body mass (Figure 2D), more time spent in light area (Figure 4A), faster locomotion (Figure 4B), more transfers (Figure 4B, right panel), and shorter latency to the first transfer (Figure 4C, right panel) in the light-dark box test are controversial in classic readouts, an aspect we address in the next point.
- *Do standard behavioral tests of mouse anxiety completely and exclusively measure mouse anxiety?* No. We argue that mice display a mixture of multiple emotional aspects in the standard behavioral tests with classic analyses. First, we showed that an emotional aspect can yield opposite behavioral phenotypes in classic analyses of standard behavioral tests (Figures 4 and 5, e.g. somatic and cognitive reactions of chronic anxiety). Second, we showed that multiple emotional aspects can couple in a single behavioral test and are mixed in corresponding classic analyses (Figure 6, e.g. distinct developmental patterns of fear and anxiety). Classically, the emotion is inferred from specific behavioral analyses (behavior-inferred emotion approach). Instead, we first considered a complete and exclusive definition of the focused emotion. Then, we quantified how much of the overall behaviors matches with the essential property inferred from the provided definition (emotion-inferred behavior approach). Our interpretation of mouse anxiety was validated in four behavioral tests (Figures 6 and 7).
- *Did fear memory support the development of chronic anxiety?* No. We observed the continuous growth of anxiety when fear reactions had long vanished (Figures 4, 5, 6 and 7).
- *Did the social deficits reflect increased anxiety?* No. The time course of social deficits led that of increased anxiety (Figures 4, 5 and 8), and social buffering with partner mice selectively rescued increased anxiety but not social deficits (Figure 11).
- *Did the trauma affect multiple behavioral aspects in parallel?* No. There is a single factor, affective bonding, commonly mediating diverse behavioral developments. Alternation of a single social

cognitive factor, social relationship, eliminated behavioral differences from mice with no traumatic experience (Figures 10 and 11). Also, among all rescuing controls, including social, environmental, or pharmacological approach (Figure 9, C to F), social buffering with stranger mice showed the best rescuing effects on diverse behaviuoral aspects (Figure 12).

- *Is there a neural substrate for the proposed psychological model?* Yes. An enhancement of an ACC-centered network was shown in DTI-based brain-wide connectome analysis (Figure 13).

Detection and identification of animal emotionality

We argue that classical behavioral analyses are too coarse to capture intricate emotional states. The traditional approach to identify animal emotionality is to test if animals show the behaviors specified by the experimental design (behavior-inferred emotion approach) [***Walf and Frye*** (***2007***)]. However, it is commonly observed that significant, robust, but inconsistent behavioral outcomes are shown in different tests with the same logic and assumptions [***Ramos*** (***2008***)]. Even if the results are consistent with the inferred behaviors, they can still be alternatively explained [***Garcia et al.*** (***2008***)]. These ambiguities reach deeply into the history of widely used behavioral tests and therefore have resulted in a considerable amount of inconclusive and seemingly paradoxical results [***Hascoët et al.*** (***2001***); ***Crusio*** (***2013***); ***Kulesskaya and Voikar*** (***2014***); ***Ennaceur*** (***2014***); ***Carobrez and Bertoglio*** (***2005***); ***Engin and Treit*** (***2008***); ***Henriques-Alves and Queiroz*** (***2016***)]. Elegantly, a proof-of-principle approach to identify animal emotionality was introduced to show that pro-social behavior in rats is driven by emphatic motivation [***Ben-AmiBartal et al.*** (***2011***)]. Here, we propose the emotion-inferred behavior approach to identify animal emotionality from standard behavioral tests which give inconclusive results when analyzed and interpreted in the traditional way.

We also introduced a simple and powerful analysis of standard behavioral tests, which allowed us to detect otherwise obscured behavioral details [***Hånell and Marklund*** (***2014***)]. Explaining subtle behavioral differences is challenging without both richer measurements and quantitative analyses [***Anderson and Perona*** (***2014***)]. The fine-scale analysis developed in our study solves this difficulty, while its utility was validated by comparing it with standard analyses which in most cases prove inconclusive; that is, for the analysis of stress incubation.

Biological mechanisms of mouse PTSD

Behavioral paradigms of laboratory rodents that simulate PTSD were established to expose the mechanistic and causal insights of long-term fear memory following acute physical stress [***Balogh et al.*** (***2002***); ***Philbert et al.*** (***2011***)] and learned depression after repeated social defeat, either directly [***Golden et al.*** (***2011***)] or through witnessing [***Warren et al.*** (***2013***); ***Sial et al.*** (***2016***)]. The diversity of PTSD models in mice is even highlighted by a paradigm of trauma-free pharmacologically-induced memory impairments in mice, which was recognized as a PTSD model and further identified the corresponding pathophysiological mechanism [***Kaouane et al.*** (***2012***)].

The phenomenon of stress incubation was observed and discussed in a few of these animal PTSD studies. Early inhibition of PTH2R (parathyroid hormone 2 receptor)-mediated TIP39 (tuberoinfundibular peptide of 39 residues) signaling in the medial amygdalar nucleus was reported to enhance the increasing fear memory following a single scrambled footshock in mice [***Tsuda et al.*** (***2015***)], although a system-level mechanism of stress incubation was limited by the sole observation of freezing time in the study. Differentiating the effects from directly physical impact, stress incubation of multiple phenotypes was more obvious in mice experiencing observational stress but not in those experiencing direct attacks [***Warren et al.*** (***2013***)]. However, an identification of post-traumatic stress incubation was challenged by significant effects of the prolonged peri-traumatic stress development from the repeated trauma induction for more than a week [***Golden et al.*** (***2011***); ***Sial et al.*** (***2016***)].

Our behavioral paradigm overcomes these limitations in identifying stress incubation process. With the behavioral foundation of our mouse paradigm, we propose that stress incubation is a process caused by the activity-induced changes of global networks from ACC after its mediation of

traumatic experience. While researches on animal emotion usually emphasize their ability to show human behavioral and physiological conditions (face validity), to reproduce pharmacological effects in human (predictive validity), and to share the same biological processes as human (construct validity) [***Calhoon and Tye*** (***2015***)], a few studies have taken the possibility of human-unique, animal-unique, and human-animal-sharing emotions under consideration [***Anderson and Adolphs*** (***2014***)]. We demonstrated human-animal-sharing emotions by the emotion-inferred behavior approach, and showed in our paradigm that affective bonding, instead of fear memory, explains stress incubation in mice.

Potential insights and applications to human PTSD

Although our study focused on stress incubation in mice, the observed psychological homology between mice and humans suggests that our paradigm can be used as simple model of psychobehavioral development in humans. Complex developmental trajectories of human PTSD symptoms were demonstrated with associated physiological and environmental regulators [***Bryant et al.*** (***2013***)], yet the combination of psychological therapy and pharmacotherapy does not provide a more efficacious treatment than psychological therapy alone for PTSD development [***Mataix-Cols et al.*** (***2017***); ***Hetrick et al.*** (***2010***)]. More than leading toward a better efficacy and lower risk in conducting psychological treatments, our research provides a foundation to test pharmacotherapies in a system-level view that integrates multiple mechanisms underlying highly diverse behavioral consequences (Figure 14). The brain heavily integrates not only external but also internal causes [***Funamizu et al.*** (***2016***); ***Larkum*** (***2013***); ***Lee et al.*** (***2015***, 2014); ***Tononi et al.*** (***2016***); ***Murugan et al.*** (***2017***); ***Zelikowsky et al.*** (***2018***); ***Kohl et al.*** (***2018***); ***Remedios et al.*** (***2017***); ***Matias et al.*** (***2017***); ***Roome and Kuhn*** (***2018***)]. Amygdala, medial prefrontal cortex, and hippocampus are the brain regions traditionally focused on in human PTSD research [***Shin et al.*** (***2006***)], with reports emphasizing the mophology of the right hippocampus [***Gilbertson et al.*** (***2002***); ***Pavić et al.*** (***2007***)]. Our data provide insights toward brain physiology on how the potentially slow and global change of brain dynamics arises from an altered dynamic in social bonding circuits through their interconnected nodes (Figures 13 and 14). The efficacy of pharmacotherapies could therefore be improved.

While much remains to be considered before clinical applications, including a better connection between our mouse results and human PTSD criteria as well as a corresponding study in humans, our study establishes a solid basis to uncover psychological theories for therapeutic strategies [***Schnyder and Cloitre*** (***2015***)]. Compared with the classic view of PTSD development as a process of complex associations [***McFarlane*** (***2010***)], we propose to consider human PTSD development as a relatively simple process with a unitary origin. While the core factor in a unitary model of human PTSD is not necessarily social bonding, we suggest a special focus on affective bonding as the core factor for patient diagnosed with witnessing PTSD.

We expect that behavioral signs of PTSD development could also be detected in humans already shortly after the traumatic event. The fine-scale behavioral analyses we introduced here provides a simple, non-invasive analytic tool to capture informative behavioral details and is not limited to laboratory animals. It opens a new window for early detection and prediction with the potential to prevent a development into PTSD.

Methods and Materials

Study design

Sample size

No statistical methods were used to predetermine sample sizes. Animal numbers were determined based on previous studies.

Rules for stopping data collection

Partner mice were expected to get minor injuries from aggressor mice during aggressive encounters, which normally should be through attack bites on the dorsal side of posterior trunk [***Takahashi***

et al. (***2015***)]. The aggressive encounter and all further experiments were terminated once (i) the partner mouse showed severe bleeding or ataxia, or (ii) the aggressor mice showed abnormal attack bites on any other body part. Partner mice that reached the criteria (i) were euthanized. Aggressor mice that reached the criteria (ii) were terminated its usage in any further experiments. If any aggressive sign (sideways threat, tail rattle, pursuit, and attack bite) was shown by the partner mouse, all further experiments with the partner mouse, aggressor mouse, and observer mouse were terminated.

Data inclusion/exclusion criteria

No data were excluded.

Outliers

No outliers were defined.

Selection of endpoints

The endpoints were prospectively selected. The criteria were approved by the Institutional Animal Care and Use Committee (IACUC) in the animal facility at the Okinawa Institute of Science and Technology (OIST) Graduate University, accredited by the Association for Assessment and Accreditation of Laboratory Animal Care (AAALAC).

Replicates

All behavioral tests were conducted in quintuplicate to octuplicate sampling replicates. All behavioral tests were conducted in single experimental cohorts. All other records were conducted in quadruplicate to septuplicate experimental cohorts.

Research objectives

The goal of this work is to identify diverse psychological aspects, temporal patterns, and associations of behavioral development in mice after a single trauma induction. Pre-specified hypotheses stated that (i) internal psychological development is already represented in behavioral details during early post-traumatic phase, while (ii) an association among trauma-induced states such as fear memory, increased anxiety, and social withdrawal explains PTSD-like behavioral development. Our data support the first pre-specified hypothesis, but not the second. All other hypotheses were suggested after initiation of the data analyses.

Research subjects or units of investigation

8-week-old male C57BL/6J mice, 16-week-old female C57BL/6J mice, and 20-week-old or older male Slc:ICR mice were used.

Experimental design

We approached the research goal by developing a novel mouse model of psychosocial trauma under highly controlled conditions (psychosocial manipulations, subjective experiences, and genetic background) and by applying fine-scale analysis to standard behavioral tests. To induce acute witnessing trauma, a pair-housed mouse observed how its partner got bullied by a larger, aggressive mouse on the day of trauma induction. After this trauma, the observer mouse was isolated and developed behavioral differences compared to control mice in the ensuing weeks. The control groups included (i) mice isolated without experiencing trauma induction, (ii) mice isolated after observing how a stranger mouse got bullied by a larger, aggressive mouse, (iii) mice isolated after exposed to a non-aggressive stranger mouse, (iv) mice which were pair-housed with their defeat partners after observing how its partner got bullied by a larger, aggressive mouse, (v) mice which were pair-housed with strangers after observing how its partner got bullied by a larger, aggressive mouse, (vi) mice isolated with their environment enriched, and (vii) mice isolated with daily injections of fluoxetine. The behavioral tests included the light-dark box test, elevated plus-maze test, open

field test, locomotor activity test, active social contact test to a female stranger, active social contact test to a male stranger, and partner-revisiting test. The non-behavioral tests included the body mass measurement, nest wall height measurement, baseline corticosterone concentration test, and *ex vivo* diffusion tensor imaging.

Randomization

Mice were from different litters. Mice were randomly paired. A focal mouse was randomly selected from each pair of mice. Mice were randomly allocated into experimental groups. Testing order among groups was counterbalanced. Strangers and aggressors were randomly assigned.

Blinding

The investigator was blinded to behavioral outcomes but not to group allocation during data collection and/or analysis.

Overview

All experimental procedures were approved by IACUC in the animal facility at the OIST Graduate University, accredited by AAALAC. In total, 467 male C57BL/6J mice (CLEA Japan, Inc.), 49 female C57BL/6J mice (CLEA Japan, Inc.), and 33 male Slc:ICR mice (Japan SLC, Inc.; retired from used for breeding) were used in this study. In CLEA Japan, nursing females were individually housed (CL-0103-2; 165×234×118 mm), while pups were separated on P21 according to gender and housed ≤15 mice per cage (CL-0104-2; 206×317×125 mm). Pups were re-arranged on P28 according to their weights and housed ≤13 mice per cage (CL-0104-2). Mice were shipped in boxes each with 10 – 30 mice to the OIST Animal Facility. In the OIST Animal Facility, mice were housed in 380×180×160-mm transparent holding cages (Sealsafe Plus Mouse DGM - Digital Ready IVC; Tecniplast Inc., Quebec, Canada) bedded with 100% pulp (FUJ9298101; Oriental Yeast Co., Ltd., Tokyo, Japan) under a 12-hr dark/light cycle (350-lux white light) at a controlled temperature of 22.7 – 22.9 ºC, humidity of 51 – 53%, and differential pressure of -14 – -8 Pa with food and water available ad libitum. Circadian time (CT) is defined to start at mid-light period and described in a 24-hr format, i.e. light off at CT 6:00.

The experimenter and caretakers wore laboratory jumpsuits, lab boots, latex gloves, face masks, and hair nets when handling mice and performing experiments. Handling of mice during the dark cycle was done under dim red light and mice were transported in a lightproof carrier within the animal facility. For mice in experimental and control groups tested on the same dates, the testing order was alternated. Surfaces of experimental apparatuses were wiped with 70% ethanol in water and dry paper tissues after testing each mouse to remove olfactory cues. Each mouse was only used for one behavioral test (in total 4 records with intervals of 6 – 21 days) to avoid confounded results due to cross-testing and to minimize measurement effects on its psychological development [***Krishnan et al.*** (***2007***)].

Pre-traumatic period (Day-21 to Day0)

To establish partnerships between mice, a male C57BL/6J mouse (focal mouse; 8 weeks) was pair-housed with another male C57BL/6J mouse (partner mouse; 8 weeks) for 3 weeks (Day-21 to Day0, with trauma induction on Day0). The partner was initially marked by ear punching. The holding cage was replaced once per week, with the last change 3 days before the traumatic event (Day-3).

To establish the territory of an aggressor mouse in its homecage, an Slc:ICR mouse (aggressor mouse; ≥20 weeks) was pair-housed with a female C57BL/6J mouse (female mouse; 16 weeks) for 3 weeks (Day-21 to Day0). The holding cage was replaced with a clean one once a week, with the last change one week before the traumatic event (Day-7).

Aggression level of aggressors was screened on Days -5, -3, -1 through intruder encounters [***Miczek et al.*** (***1978***)] toward different screening mice to determine appropriate aggressors to be used for trauma induction on Day0. Aggression screening was carried out in the behavior testing

room at 22.4 – 23.0 ºC, 53 – 58% humidity, -4 – -3 Pa differential pressure, and 57.1 dB(C) ambient noise level during the light period (CT 4:00 – 6:00) with 350-lux white light. After the female and pups with the aggressor were taken out of their homecage and kept in a clean holding cage in the behavior testing room, a 3-min aggression screening was started after a male C57BL/6J mouse (screening mouse; 10 weeks) was brought into the homecage of the aggressor, followed by covering the cage with a transparent acrylic lid. During screening, the aggressor freely interacted with the screening mouse. The aggressor was brought back to the holding room after the screening mouse was taken away from the aggressor's homecage and the female and pups were brought back to its homecage right after screening. Aggressors were selected for trauma induction on Day0 if they showed biting attacks on all of these screening days and the latencies to the initial bites on Day-3 and Day-1 were less than 20 s.

Trauma induction (Day0)

The following experimental assay emotionally introduced an acute traumatic experience in mice through a social process. The setup was the aggressor's homecage, divided into an 80×180-mm auditorium zone and a 300×180-mm battle arena by the insertion of a stainless-steel mash with 8×8-mm lattices. The cage was covered with a transparent acrylic lid. The behavioral procedure was carried out in the behavior testing room during CT 4:00 – 6:00, with 3 – 5 experiments done in parallel.

After the female and pups with the aggressor were taken out of their homecage, a divider was inserted into the aggressor's homecage, allowing the aggressor to freely behave in the battle arena, but not to enter the auditorium zone. A 5-min aggression encounter session started after the focal mouse was brought to the auditorium zone and its partner to the battle arena. Tail rattling counts of the focal mouse during aggressive encounter were recorded by experimenter. The aggressive encounter session was followed by a 5-min stress infiltration session, in which the partner was brought to the focal mouse in the auditorium zone, while the aggressor remained in the battle arena. Right after the stress infiltration session, both focal mouse and its partner were brought back to their homecage in the behavior testing room for a 10-min resting period. The procedure was repeated 5 times with different aggressors. During each resting session, the aggressor stayed in its homecage without the divider before its next intruder encounter. Each aggressor had 3 – 5 encounters with resting periods of 10 – 30 min. After the 5th aggression encounter session, the focal mouse was placed back in its homecage where the nest had been razed, and brought back to the holding room. Partners from different pairs were brought to a new holding cage and housed in groups of 3 – 5 per cage. Right after the last intruder encounter for each aggressor, the female and pups were brought back to the homecage and returned to the holding room together with the aggressor.

Post-traumatic period (Day0 to Day28)

To investigate the behavior of focal mice after trauma induction (now called Partner-observing mice, Figure 1B), they were housed individually for 4 weeks after the procedure (Day0 to Day28). No environmental enrichment was provided, except to the Environment-enriched mice, and the holding cage was not changed during social isolation.

Control experiments

To differentiate behavioral consequences of the emotionally traumatic experience from consequences of social isolation, a control group of mice had their partners taken away and their nests razed during body weighing on Day0 without trauma induction (No-scenario-isolated mice, Figure 1C).

To test the influence of social relationship on the emotionally traumatic experience, a control group of mice witnessed the traumatic events toward stranger mice of the same strain, gender, and

age instead (Stranger-observing mice, Figure 9A). In each iteration of the aggression encounter, stress infiltration, and resting period, a different stranger mouse was presented.

To identify the impacts of aggression during trauma induction, a control group of mice experienced exposure to strangers of the same strain, gender, and age, instead of the aggressor mice for trauma induction (Stranger-exposed mice, Figure 9B).

To examine the potential reversal effects of social support on the emotionally traumatic experience, a control group of mice was kept pair-housed with their attacked partners after trauma induction (Partner-buffered mice, Figure 9C).

To further test the critical component of social relationship in the potential social support reversal, a control group of mice was kept pair-housed but with a stranger mouse after trauma induction (Stranger-buffered mice, Figure 9D).

To characterize potential reversal effects through environmental factors besides social factors, a control group of mice was housed individually with environmental enrichment, provided with a pair of InnoDome™ and InnoWheel™ (Bio-Serv, Inc., Flemington, NJ, USA) and a Gummy Bone (Petite, Green; Bio-Serv, Inc.), after trauma induction (Environment-enriched mice, Figure 9E).

To demonstrate predictive validity of potential treatment on stress by an antidepressant, a control group of mice was intraperitoneally injected with fluoxetine (2 µl/g of 10 mg/ml fluoxetine hydrochloride dissolved in saline, i.e. 20 mg/kg; F132-50MG; Sigma-Aldrich, Inc., Saint Louis, MO, USA) once per day at CT 1:00 – 2:00 after trauma induction (FLX-treated mice, Figure 9F).

Body mass and nest wall height

In the holding room, body masses of all individuals were recorded on Days -7, 0, 1, 7, 28, while the heights of nest walls built by each individual were recorded on Days 1, 7, 28. The height of the nest wall was measured with 5-mm resolution using a transparent acrylic ruler, while the mouse was weighed with 10-mg resolution on a balance. Mice were placed back in their homecages right after recording.

Light-dark box test

The light-dark box test is an experimental assay to measure anxiety in rodents [***Crawley and Goodwin*** (***1980***)], designed to evaluate their natural aversion to brightly lit areas against their temptation to explore. The light-dark box setup consisted of two connected 200×200×250-mm non-transparent PVC boxes, separated by a wall with a 50×30-mm door. The boxes were covered with lids with white and infrared LED light illumination for the light and dark areas, respectively, and CCD cameras in the centers (4-chamber system; O'Hara & Co., Ltd., Tokyo, Japan). The floors of the boxes were white, while the walls of the boxes were white for the light area and black for the dark area. Uniform illumination in the light area was 550 lux. Behavioral tests were carried out on Days -7, 1, 7, and 28 in the behavior testing room at 22.7 – 23.0 °C, 51 – 54% humidity, -11 – -9 Pa differential pressure, and 53.6 dB(C) ambient noise level during dark period (CT 6:00 – 8:00).

After habituation for 10 min individually in the homecage in the behavior testing room in darkness, the focal mouse was transferred to the dark area through a 50×50-mm side door. A 5-min behavior record was started right after the side door of dark area was closed and the door between light and dark areas was opened. Locomotion was recorded 2-dimensionally at 15 Hz from top-view with CCD video cameras. Right after recording, the mouse was returned to its homecage, and brought back to the holding room.

Elevated plus-maze test

The elevated plus-maze test is an experimental assay to measure anxiety in rodents [***Pellow et al.*** (***1985***)], designed to evaluate their natural fear of falling and exposure against their temptation to explore. The elevated plus-maze setup consisted of a gray PVC platform raised 500 mm above the ground (single maze system; O'Hara & Co., Ltd.). The platform was composed of a 50×50-mm square central platform, two opposing 50×250-mm open arms, and two opposing 50×250-mm

closed arms with 150-mm semi-transparent walls. Each of the two open arms emanated at 90° to each of the two closed arms, and vice versa. The apparatus was installed in a soundproof box with white fluorescent lamp illumination (20 lux) and ventilators. Behavioral tests were carried out on Days -7, 1, 7, 28 in the behavior testing room at 22.8 – 23.0 ºC, 53 – 56% humidity, -13 – -11 Pa differential pressure, and 52.1 dB(C) ambient noise level during dark period (CT 8:00 – 10:00).

After habituation for 10 min individually in the homecage in the behavior testing room in darkness, the focal mouse was brought to the central platform of the elevated plus-maze, facing the open arm on the opposite side from the door of the soundproof box. A 5-min behavior recording was started right after the door of the soundproof box was closed. Locomotion was recorded 2-dimensionally at 15 Hz from top-view with a CCD video camera installed above the center of the central platform. Delineated entrances to open and closed arms were defined at 50 mm from the center of the central platform. Right after recording, the mouse was placed back in its homecage, and brought back to the holding room.

Open field test

The open field test is an experimental assay to measure anxiety in rodents [***Hall and Ballachey (1932)***], designed to evaluate their spontaneous activity under a gradient of spatial uncertainty (high in the field center and low along the walls and at the corners of the field). The open field setup consisted of a 400×400×300-mm non-transparent gray PVC box with no cover, installed in a soundproof box with white LED light illumination and ventilators (2-chamber system; O'Hara & Co., Ltd.). Behavioral tests were carried out on Days -7, 1, 7, 28 in the behavior testing room at 22.8 – 23.0 ºC, 53 – 56% humidity, -13 – -11 Pa differential pressure, and 56.7 dB(C) ambient noise level during dark period (CT 8:00 – 10:00).

After habituation for 10 min individually in the homecage in the behavior testing room in darkness, the focal mouse was brought to the center of the open field arena under 20-lux uniform illumination, facing the wall on the opposite side from the door of the soundproof box. A 5-min behavior recording was started right after the door of the soundproof box was closed. Locomotion was recorded 2-dimensionally at 15 Hz from top-view with a CCD video camera installed above the center of the open field arena. Vertical activity of exploratory rearing behavior was recorded by the blocking of invisible infrared beams created and detected by photocell emitters and receptors, respectively, positioned 60 mm high on the walls of the open field box. A delineated center region was defined as the central 220×220 mm area. Right after recording, the mouse was placed back in its homecage, and returned to the holding room.

Locomotor activity test

The locomotor activity test is an experimental assay to measure spontaneous activity of rodents in an environment without an experimentally designed stressor. The locomotor activity setup consisted of a 200×200×250 mm non-transparent covered PVC box with infrared LED illumination and a CCD camera in the center (the dark area of the light-dark box setup, while the door between the light and dark areas was closed and fixed). The floor of the box was embedded with bedding material from the homecage of the focal mouse, while the walls of the box were black. Behavioral test was carried out on Days -7, 1, 7, 28 in the behavior testing room at 22.7 – 23.0 ºC, 51 – 54% humidity, -11 – -9 Pa differential pressure, and 53.6 dB(C) ambient noise level during dark period (CT 6:00 – 8:00).

After habituation for 30 min individually in the behavior testing box, a 1-hr behavior recording was started. The behavior testing box was not covered completely in order to allow air circulation. Locomotion was recorded 2-dimensionally at 15 Hz from top-view with the CCD video camera. Right after recording, the mouse was returned to its homecage, and brought back to the holding room.

Active social contact test

The active social contact test (also known as "social interaction test", but to be distinguished with the one-session test using an open field with a social target freely behaving in the field [***Arakawa et al.*** (***2014***)] or the one-session test placing a social target-containing cylinder into the center of the testing subject's homecage for social instigation [***Tsuda and Ogawa*** (***2012***)]) is a 2-session experimental assay to measure social motivation in rodents [***Berton*** (***2006***)]. The setup consists of a 400×400×300-mm non-transparent gray PVC box with no cover, installed in a soundproof box with 20-lux white LED illumination and ventilators. A 60×100×300-mm stainless-steel chamber with wire grid sides was placed in the center of the wall on the opposite side from the door of the soundproof box. The wire grid had 8×8 mm lattices at a height of 10 – 60 mm from the bottom. An ultrasound microphone (CM16/CMPA; Avisoft Bioacoustics, Glienicke, Germany) with an acoustic recording system (UltraSoundGate; Avisoft Bioacoustics) was hung outside the chamber, 100 mm above the ground. Behavioral tests were carried out on Days -7, 1, 7, 28 in the behavior testing room at 22.8 – 23.0 ºC, 53 – 56% humidity, -13 – -11 Pa differential pressure, and 56.7 dB(C) ambient noise level during dark period (CT 8:00 – 10:00).

The social target used for active social contact tests was either a male or a female C57BL/6J mouse (18 weeks), pair-housed with a partner of the same strain, gender, and age for more than 2 weeks before the tests. The social target was adapted to the experimental protocol one day before the tests in the behavior testing room during dark period (CT 8:00 – 9:00): After habituation for 5 min individually in the homecage in the soundproof box under 20-lux uniform illumination, the social target was brought into the chamber in the open field arena under 20 lux uniform illumination. A male C57BL/6J mouse (11–16 weeks; from partners of No-scenario-isolated mice in previous experiment) was then brought to the open field arena for a 2.5-min spontaneous exploration and interaction with the social target. The social target was then brought back to its homecage in the soundproof box under 20-lux uniform light for a 5-min rest. The social interaction procedure was repeated with a different male C57BL/6J mouse right afterward. After the social target had interacted with 4 different mice, it was returned to its homecage and brought back to the holding room.

The focal mouse experienced active social contact tests with different social targets on different recording days (Days -7, 1, 7, 28), while different focal mice were tested with the same social target on the same recording day (5 – 10 records). The social target remained in its homecage in a soundproof box under 20-lux uniform illumination before and between each test. A delineated interaction zone was taken as the region within 80 mm of the edges of the chamber. Social approaches of the focal mouse poking its nose toward the social target were recorded manually using the event recording software, tanaMove ver0.09 (http://www.mgrl-lab.jp/tanaMove.html).

Partner-revisiting test

The partner-revisiting test is a memory-based experimental assay to measure social bonding in rodents (sharing similar concept of "familiar *v.s.* novel social target recognition", but to be distinguished with the three-chamber paradigm test [***Nadler et al.*** (***2004***)]). The partner-revisiting setup was the uncovered homecage of the focal mouse, installed in a soundproof box with white LED illumination and ventilators (O'Hara & Co., Ltd., Tokyo, Japan). The long sides of the homecage were parallel to the door of soundproof box. The partner-revisiting test was carried out on Day28 in the behavior testing room at 22.8 – 23.0 ºC, 53 – 56% humidity, -13 – -11 Pa differential pressure, and 56.7 dB(C) ambient noise level during light period (CT 4:00 – 6:00) with 350-lux light intensity.

The previously separated partner of the focal mouse, being a social target in the test, was initially sedated with 3%v/v isoflurane in oxygen, and then anesthetized by intraperitoneal (i.p.) injection of a mixture of medetomidine (domitor, 3%v/v in saline, 0.3 mg/kg), midazolam (dormicum, 8%v/v in saline, 4 mg/kg), and butorphanol (vetorphale, 10%v/v in saline,5 mg/kg). Also, a stranger mouse (15 weeks; a separated partner of a Partner-observing or Buffered mouse for testing a No-scenario-isolated, Stranger-observing, or Stranger-exposed mouse, and vice versa) was anesthetized as an

alternative social target. Both anesthetized mice were kept on a heating pad at 34ºC (B00O5X4LQ2; GEX Co., Ltd., Osaka, Japan) to maintain their body temperatures before the test.

The focal mouse was brought to a clean, uncovered holding cage in the soundproof box under 50-lux uniform illumination for 5-min habituation, while its homecage was placed in another soundproof box under 50-lux uniform light. During habituation of the focal mouse, the anesthetized social targets were injected with atipamezole hydrochloride (antisedan; 6%v/v in saline for 0.3 mg/kg, i.p.) to induce recovery from anesthesia. During the waking-up period, the social targets were still immobilized and not able to actively interact with the focal mouse during the following recording, but showed enough social cues to be attractive for the focal mouse. The immobilized social targets were then placed in the homecage of the focal mouse with their nose pointing toward the center of the short side of the wall (10 mm of nose-to-wall distance) with their bellies facing the door of the soundproof box. After habituation, the focal mouse was brought to the center of its homecage, facing the long side of the homecage wall on the opposite side from the door of soundproof box. A 10-min behavior record started right after the door of the soundproof box was closed. Locomotion was recorded 2-dimensionally at 15 Hz from top-view with a CCD video camera installed above the center of the homecage. Right after recording, social targets were taken out of the focal mouse's homecage and the focal mouse was brought back to the holding room.

Social contacts including sniffing, allogrooming, and pushing of the focal mouse toward each of the social targets were recorded manually using the event recording software, tanaMove ver0.09 (http://www.mgrl-lab.jp/tanaMove.html).

Baseline plasma corticosterone concentration test

The baseline plasma corticosterone (CORT) concentration test is a competitive-inhibition enzyme-linked immunosorbent assay (ELISA) to measure physiological stress level in rodents, designed to quantitatively determinate CORT concentrations in blood plasma. The sample collection was carried out on Days -7, 1, 7, 28 in the behavior testing room at 22.4 – 23.0 ºC, 53 – 58% humidity, -4 – -3 Pa differential pressure, and 57.1 dB(C) ambient noise level during CT 4:00 – 6:00 with 350-lux white light.

After habituation for 30 min individually in the homecage in the behavior testing room, the mouse was initially sedated with 3%v/v isoflurane in oxygen. Six drops of blood from the facial vein pricked by a 18G needle were collected in a EDTA-lined tube [K2 EDTA (K2E) Plus Blood Collection Tubes, BD Vacutainer; Becton, Dickinson and Company (BD), Franklin Lakes, NJ, USA] and kept on ice. Right after collection, the mouse was returned to its homecage, and brought back to the holding room. Whole blood samples were then centrifuged (MX-300; Tomy Seiko Co., Ltd., Tokyo, Japan) at 3,000 rpm for 15 min at 4°C. Plasma supernatant was decanted and kept at -80°C until the measurement on Day 29.

CORT concentrations in blood plasma were tested with Mouse Corticosterone (CORT) ELISA Kit (MBS703441, 96-Strip-Wells; MyBioSource, Inc., San Diego, USA; stored at 4°C before use) on Day 29. All reagents [assay plate (96 wells, pre-coated with goat-anti-rabbit antibody), standards (0, 0.1, 0.4, 1.6, 5, and 20 ng/ml of CORT), rabbit-anti-CORT antibody, HRP-conjugated CORT, concentrated wash buffer (20x phosphate-buffered saline (PBS)), 3,3',5,5'-tetramethylbenzidine (TMB) color developing agent (substrates A and B), and TMB stop solution] and samples were brought to room temperature for 30 min before use. Collected plasma samples after thawing were centrifuged again (MX-300; Tomy Seiko Co.) at 3,000 rpm for 15 min at 4°C. 20 μl of standard or sample was added per well, assayed in duplicate, with blank wells set without any solution. After 20 μl of HRP-conjugated CORT was added to each well except to the blank wells, 20 μl of rabbit-anti-CORT antibody was added to each well and mixed. After incubation for 1 hour at 37°C, each well was aspirated and washed, repeated for 3 times, by filling each well with 200 μl of wash buffer (diluted to 1x PBS) using a squirt bottle, standing for 10 s, and completely removing liquid at each step. After the last wash and the removal of any remaining wash buffer by decanting, the plate was inverted and blotted against clean paper towels. After TMB color developing agent (20 μl of substrate A and 20 μl of substrate

B) was added to each well, mixed, and incubated for 15 min at 37°C in dark, 20μl of TMB stop solution was added to each well and mixed by gently tapping the plate. The optical density (O.D.) of each well was determined, within 10 min, using a microplate reader (Multiskan GO; Thermo Fisher Scientific, Inc., Waltham, MA, USA) measuring absorbance at 450 nm, with correction wavelength set at 600–630 nm.

CORT concentrations were calculated from the O.D. results using custom scripts written in MATLAB R2015b (MathWorks). Two O.D. readings of each standard and sample were averaged and background corrected,

$$X = \langle O.D. \rangle - \langle O.D. \rangle_{\text{blank}} \ .$$

A standard curve was determined by a four parameter logistic (4PL) regression fitting the equation

$$\rho_{CORT}(X_{\text{standard}}) = d + \frac{a-d}{1+(\frac{X_{\text{standard}}}{c})^b} \ ,$$

where ρ_{CORT} is the CORT concentration, a is the minimum asymptote, b is the Hill's coefficient, c is the inflection point, and d is the maximum asymptote. CORT concentrations of the samples were calculated from the fitted 4PL equation with respect to X_{sample}.

Ex vivo diffusion tensor imaging

Ex vivo diffusion tensor imaging (DTI) is a magnetic resonance imaging (MRI) technique to determinate structural information about tissues [***Basser et al.*** (***1993***)], designed to measure the restricted diffusion of water in tissue. The sample collection was carried out on Day 28 in the necropsy room at 22.4 - 22.5 ºC, 53 - 54 % humidity, and 10 - 12 Pa differential pressure during CT 4:00 - 6:00 with 750-lux white light.

After mice were brought individually in their homecages to the necropsy room, they were initially sedated with 3%v/v isoflurane in oxygen, then deeply anaesthetized with a ketamine-xylazine mixture (>30 μl/g body weight of 100 mg/ml ketamine and 20 mg/ml xylazine), and perfused transcardially. The perfusates, in a two-step procedure, were (i) 20 ml of ice cold 1x phosphate-buffered saline (PBS), and (ii) 20 ml of ice cold 4% paraformaldehyde, 0.2% sodium meta-periodate, and 1.4% lysine in PBS. Mouse skull including the brain was removed and stored in the perfusate (ii) at 4 ºC for 2 weeks. Each skull with the brain was then transferred into 2 mM gadolinium with diethylenetriaminepentaacetic acid (Gd-DTPA) and 0.5% azide in PBS for 2 weeks.

Isolated fixed brains within the skulls were positioned in an acrylic tube filled with fluorinert (Sumitomo 3M Ltd., Tokyo, Japan) to minimize the signal intensity attributable to the medium surrounding the brain during MRI scanning. All MRI was performed with an 11.7-T MRI system (BioSpec 117/11; Bruker Biospec, Ettlingen, Germany) using ParaVision 6.0.1 software (Bruker Biospec, Ettlingen, Germany) for data acquisition. The inner diameter of the integrated transmitting and receiving coil (Bruker Biospec, Ettlingen, Germany) was 35 mm for the *ex vivo* MRI. DTI data were acquired by using a 3-D diffusion-weighted spin-echo imaging sequence, with repetition time (TR) = 267 ms, echo time (TE) = 18.5 ms, *b*-value = 2,000 s/mm^2, and 30 non-collinear directions. Five T2-weighted measurements were acquired together with DTI, for one every 6 diffusion measurements. The acquisition matrix was 216×216×168 over a 27.0×27.0×21.0 mm^3 field of view, resulting in a native isotropic image resolution of 125 μm. Total acquisition time was 96 hr.

MRI data was processed using custom scripts written in MATLAB R2015b (MathWorks). All 30 DTI and 5 T2 3-D images were masked by thresholding at the half of mean values of diffusion weights for each voxel and omiting clusters smaller than 10 voxels. After diffusion tensor of each voxel was estimated by solving the Stejskal-Tanner equation through linear regression [***Hrabe et al.*** (***2007***)], the 3 eigenvalues (λ_1, λ_2, and λ_3) with respect to the 3 axes of the diffusion ellipsoid (the longest, middle, and shortest axes, respectively) were calculated by eigenvalue decomposition of

the diffusion tensor. Four focused DTI-based measures [*Mori* (*2007*)] are the mean diffusivity (MD) that represents membrane density

$$MD = \langle \lambda \rangle = \frac{\lambda_1 + \lambda_2 + \lambda_3}{3} \ ,$$

axial diffusivity (AD) that represents neurite organization

$$AD = \lambda_1 \ ,$$

radial diffusivity (RD) that reprsents myelination

$$RD = \frac{\lambda_2 + \lambda_3}{2} \ ,$$

and fractional anisotropy (FA) that represents average microstructural integrity

$$FA = \sqrt{\frac{3 \times \left[(\lambda_1 - \langle \lambda \rangle)^2 + (\lambda_2 - \langle \lambda \rangle)^2 + (\lambda_2 - \langle \lambda \rangle)^2\right]}{2 \times \left(\lambda_1^2 + \lambda_2^2 + \lambda_3^2\right)}} \ .$$

After the registeration of these 3-D DTI-based brain maps to a template brain atlas (DSURQE 40-μm C57Bl/6J mouse MRI brain atlas; https://wiki.mouseimaging.ca/display/MICePub/Mouse+Brain+Atlases), mean values of these DTI-based quantities were identified in a total of 244 brain regions (Figure 3) for each individual. Based on the FA maps, DTI-based long-range fiber tracking from a focal seed region (Figure 13B) was calculated with 2 samplings, distance of forward fiber in one step = 50 μm, and thresholds of minimal fiber length = 750 μm, maximal fiber length = 75,000 μm, maximal fiber deviation angle = 57.3º, and minimal FA for keeping tracking = 0.4.

Video image process

Video image data was processed using custom scripts written in MATLAB R2015b (MathWorks). Each video frame from a recorded AVI video file was read as a 2-dimensional matrix with an 8-bit gray scale. Each of these matrices was then divided by a background matrix read from a TIF image file of the background taken before bringing the test mouse to the setup. The centroid of the area with non-one values in each matrix ratio was taken as the position of the mouse at this specific time point. Speed was calculated as the distance between temporally adjacent positions multiplied by 15 (15-Hz recording). Freezing periods were sorted out if the area of the mouse body between temporally adjacent frames was less than 20 mm^2.

Audio signal process

Audio signal data was processed with custom scripts written in MATLAB R2015b (MathWorks). Each recorded WAV audio file was read and transformed into a spectrogram using fast Fourier transform with non-overlapping 0.4-ms time windows. To identify the time segments with ultrasonic vocalization signals, recordings were thresholded at a power spectral density (PSD) $\geq$-75 dB/Hz, and time segments with averaged PSD between 0–50 kHz higher than that between 50–120 kHz were removed. The duration of remaining time segments was calculated.

Statistical analysis

Numerical data were analyzed with custom scripts written in MATLAB R2015b (MathWorks). Statistical significance of the difference between 2 mean values was estimated with two-tailed, two-sample Student's *t*-test, except of DTI quantities which were estimated with one-tailed, two-sample Student's t-test. Statistical significance of the difference between 2 median values (vocalization analysis; Figure 8F) was estimated using one-tailed Mann–Whitney *U* test.

To capture fine-scale behavioral details of location within the light-dark box and the elevated plus-maze (Figures 4 and 5), we computed T(x), the cumulative probability of finding position $\leq$x, for each individual (light traces) for all measured locations (a collection of locations from all

mice for the statistics). We then show the average across the control group (bold blue trace) and the Partner-observing group (bold red trace). We compared the averages of each group with a two-tailed, two-sample Student's t-test and plot the resulting p-values, presented as -log(p), the negative logarithm of p-values. We also show the box plot (the minimum, lower quartile, median, upper quartile, and maximum) of -log(p) values collapsed across all measured locations. To capture the fine- scale behavioral details of speed, we followed a similar procedure as above, but with U(v), the cumulative distribution function of finding speed ≤v.

To evaluate the uncertainty of the percentage for each tail rattle count (Figure 10A), we created 10,000 bootstrapped data sets where each sample was randomly picked with replacement from the original data set. Each bootstrapped data set had the same sample size as the original data set. The standard error was taken as the standard deviation of the bootstrapped percentages for a tail rattle count. A similar procedure was carried out to evaluate the standard error of mean for the percentage of time spent in each behavior in the partner-revisiting test (Figure 10H), where each sample of the bootstrapped data sets was a set of the percentages of the three classified behaviors (partner concern, stranger concern, and non-social activity/sniffing at social targets) from a mouse record. Standard errors of means for other results were estimated with the formula $\sigma/\sqrt{n}$, where σ is the sample standard deviation and n is the sample size.

Video supplements

Figure 7-video supplement 1. Social apathy is an observed behavioral characteristic of Partner-observing mice. Examples of 30-s recordings during the social session in the female stranger test on Day1. First scene, No-scenario-isolated mouse; Second scene, Partner-observing mouse.

Figure 9-video supplement 1. Illustration of behavioral characteristics that were specific to observer mice during trauma induction when their partners were attacked. First scene, tail rattling during aggressive encounter; Second scene, tail rattling during aggressive encounter (4x slower); Third scene, hiding under bedding material with the partner during resting. These behaviors were not observed if a stranger mouse got attacked.

Figure 9-video supplement 2. Illustration of rebound reaction of a Partner-observing mouse to its previously pair-housed partner during the partner-revisiting test.

Acknowledgements

We thank Tsuyoshi Koide (NIG, Japan), Aki Takahashi (University of Tsukuba), Teruhiro Okuyama (MIT), Charles Yokoyama (RIKEN BSI), Ai Koizumi (CiNet), and Tsai-Wen Chen (National Yang-Ming University) for comments, Tadashi Yamamoto (OIST) for sharing behavior testing setups, and Steven D. Aird (OIST) for editing the manuscript.

We acknowledge a JSPS KAKENHI Grant (JP 16J10077) by DC1 Student Research Fellowship to R.X.L. and OIST internal funding to B.K. The funders had no role in study design, data collection and interpretation, or the decision to submit the work for publication.

R.X.L. conceptualized the study, designed the research, performed experiments, analyzed data, interpreted results, wrote the original draft, and revised the article; G.J.S. advised on data analysis and revised the article; B.K. advised on research design and revised the article.

The authors declare no competing financial interests.

References

Adler L, Kunz M, Chua H, Rotrosen J, Resnick S. Attention-deficit/hyperactivity disorder in adult patients with posttraumatic stress disorder (PTSD): Is ADHD a vulnerability factor? Journal of Attention Disorders. 2004; 8:11–16.

Anderson DJ. Circuit modules linking internal states and social behaviour in flies and mice. Nature Reviews Neuroscience. 2016; 17:692–704.

Anderson DJ, Adolphs R. A framework for studying emotions across species. Cell. 2014; 157(1):187–200.

Anderson DJ, Perona P. Toward a science of computational ethology. Neuron. 2014; 84(1):18–31.

Andrews B, Brewin CR, Philpott R, Stewart L. Delayed-onset posttraumatic stress disorder: a systematic review of the evidence. American Journal of Psychiatry. 2007; 164:1319–1326.

Arakawa T, Tanave A, Ikeuchi S, Takahashi A, Kakihara S, Kimura S, et al. A male-specific QTL for social interaction behavior in mice mapped with automated pattern detection by a hidden Markov model incorporated into newly developed freeware. Journal of neuroscience methods. 2014; 234:127–134.

Archer J. Tests for emotionality in rats and mice: a review. Animal behaviour. 1973; 21:205–235.

Balogh SA, Radcliffe RA, Logue SF, Wehner JM. Contextual and cued fear conditioning in C57BL/6J and DBA/2J mice: context discrimination and the effects of retention interval. Behavioral neuroscience. 2002; 116:947.

Basser PJ, Mattiello J, Turner R, Bihan DL. Diffusion tensorecho-planar imaging of human brain. In: ; 1993. p. 584.

Ben-AmiBartal I, Decety J, Mason P. Empathy and pro-social behavior in rats. Science. 2011; 334:1427–1430.

Ben-AmiBartal I, Rodgers DA, Sarria MSB, Decety J, Mason P. Pro-social behavior in rats is modulated by social experience. Elife. 2014; 3:01385.

Ben-AmiBartal I, Shan H, Molasky NM, Murray TM, Williams JZ, Decety J, et al., Anxiolytic treatment impairs helping behavior in rats; 2016. Frontiers in psychology, 7, 850 .

Berton O. Essential role of BDNF in the mesolimbic dopamine pathway in social defeat stress. Science. 2006; 311(5762):864–868.

Bryant RA, Creamer M, O'donnell M, Forbes D, Mcfarlane AC, Silove D, et al. Acute and chronic posttraumatic stress symptoms in the emergence of posttraumatic stress disorder: a network analysis. JAMA psychiatry. 2017; 74:135–142.

Bryant RA, O'donnell ML, Creamer M, Mcfarlane AC, Silove D. A multisite analysis of the fluctuating course of posttraumatic stress disorder. JAMA psychiatry. 2013; 70:839–846.

Burkett JP, Andari E, Johnson ZV, Curry DC, Waal FBD, Young LJ. Oxytocin-dependent consolation behavior in rodents. Science. 2016; 351:375–378.

Calhoon GG, Tye KM. Resolving the neural circuits of anxiety. Nature neuroscience. 2015; 18:1394–1404.

Carobrez AP, Bertoglio LJ. Ethological and temporal analyses of anxiety-like behavior: the elevated plus-maze model 20 years on. Neuroscience & Biobehavioral Reviews. 2005; 29(8):1193–1205.

Chung MC, Farmer S, Grant K, Newton R, Payne S, Perry M, et al. Coping with post-traumatic stress symptoms following relationship dissolution. Stress and Health. 2003; 19:27–36.

Cloninger C. Anxiety and theories of emotion. Handbook of. 1988; 2:1–29.

Cohen S, Wills TA. Stress, social support, and the buffering hypothesis. Psychological bulletin. 1985; 98(2):310.

Crawley J, Goodwin FK. Preliminary report of a simple animal behavior model for the anxiolytic effects of benzodiazepines. Pharmacology Biochemistry and Behavior. 1980; 13:167–170.

Crusio WE. The genetics of exploratory behavior. Behavioral Genetics of the House Mouse. 2013; 1:148–154.

Cryan JF, Holmes A. The ascent of mouse: advances in modelling human depression and anxiety, vol. 4; 2005.

Davis M. Sensitization of the acoustic startle reflex by footshock. Behav Neurosci. 1989; 103:495–503.

DeMorrow S, Role of the Hypothalamic–Pituitary–Adrenal Axis in Health and Disease.; 2018.

Diven K. Certain determinants in the conditioning of anxiety reactions. The Journal of Psychology. 1937; 3(1):291–308.

DSM-5. Diagnostic and statistical manual of mental disorders (DSM-5). In: American Psychiatric Association; 2013. .

DSM-III. Diagnostic and Statistical Manual of Mental Disorders (DMS III). In: American Psychiatric Association; 1980. .

Ehlers A, Clark DM. A cognitive model of posttraumatic stress disorder. Behaviour research and therapy. 2000; 38:319–345.

Engin E, Treit D. The effects of intra-cerebral drug infusions on animals' unconditioned fear reactions: a systematic review, vol. 32; 2008.

Ennaceur A. Tests of unconditioned anxiety—pitfalls and disappointments. Physiology & behavior. 2014; 135:55–71.

Fischer AG, Ullsperger M. An Update on the Role of Serotonin and its Interplay with Dopamine for Reward, vol. 11; 2017.

Funamizu A, Kuhn B, Doya K. Neural substrate of dynamic Bayesian inference in the cerebral cortex. Nature neuroscience. 2016; .

Garcia AMB, Martinez RCR, Morato S. Preference for the light compartment of a light/dark cage does not affect rat exploratory behavior in the elevated plus-maze. Psychology & Neuroscience. 2008; 1(1):73–80.

Gilbertson MW, Shenton ME, Ciszewski A, Kasai K, Lasko NB, Orr SP, et al. Smaller hippocampal volume predicts pathologic vulnerability to psychological trauma. Nature neuroscience. 2002; 5(11).

Golden SA, Iii HEC, Berton O, Russo SJ. A standardized protocol for repeated social defeat stress in mice. Nature protocols. 2011; 6:1183–1191.

Goto T, Kubota Y, Tanaka Y, Iio W, Moriya N, Toyoda A. Subchronic and mild social defeat stress accelerates food intake and body weight gain with polydipsia-like features in mice. Behavioural brain research. 2014; 270:339–348.

Grupe DW, Nitschke JB. Uncertainty and anticipation in anxiety: an integrated neurobiological and psychological perspective. Nature Reviews Neuroscience. 2013; 14:488–501.

Hall C, Ballachey EL. A study of the rat's behavior in a field. A contribution to method in comparative psychology; 1932.

Hånell A, Marklund N. Structured evaluation of rodent behavioral tests used in drug discovery research, vol. 8; 2014.

Hascoët M, Bourin M, Dhonnchadha BAN. The mouse ligth-dark paradigm: a review, vol. 25; 2001.

Hayes JP, Vanelzakker MB, Shin LM. Emotion and cognition interactions in PTSD: a review of neurocognitive and neuroimaging studies; 2012.

Henriques-Alves AM, Queiroz CM. Ethological evaluation of the effects of social defeat stress in mice: beyond the social interaction ratio, vol. 9; 2016.

Hetrick SE, Purcell R, Garner B, Parslow R. Combined pharmacotherapy and psychological therapies for post traumatic stress disorder (PTSD). The Cochrane Library; 2010.

Houston FP, Stevenson GD, McNaughton BL, Barnes CA. Effects of age on the gener- alization and incubation of memory in the F344 rat. Learning &. Memory; 1999.

Hrabe J, Kaur G, Guilfoyle DN. Principles and limitations of NMR diffusion measurements. Journal of medical physics/Association, vol. 32; 2007.

Ishiyama S, Brecht M. Neural correlates of ticklishness in the rat somatosensory cortex. Science. 2016; 354(6313):757–760.

Kaouane N, Porte Y, Vallée M, Brayda-Bruno L, Mons N, Calandreau L, et al. Glucocorticoids can induce PTSD-like memory impairments in mice. Science. 2012; 335:1510–1513.

Knox D, George SA, Fitzpatrick CJ, Rabinak CA, Maren S, Liberzon I. Single prolonged stress disrupts retention of extinguished fear in rats. Learning & memory. 2012; 19(2):43–49.

Kogan JH, Frankland PW, Silva AJ. Long-term memory underlying hippocampus-dependent social recognition in mice. Hippocampus. 2000; 10:47–56.

Kohl J, Babayan BM, Rubinstein ND, Autry AE, Marin-Rodriguez B, Kapoor V, et al. Functional circuit architecture underlying parental behaviour. Nature. 2018; 556(7701):326.

Krishnan V, Han MH, Graham DL, Berton O, Renthal W, Russo SJ, et al. Molecular adaptations underlying susceptibility and resistance to social defeat in brain reward regions. Cell. 2007; 131:391–404.

Kulesskaya N, Voikar V. Assessment of mouse anxiety-like behavior in the light–dark box and open-field arena: role of equipment and procedure. Physiology & behavior. 2014; 133:30–38.

Kumar V, Bhat ZA, Kumar D. Animal models of anxiety: a comprehensive review. Journal of pharmacological and toxicological methods. 2013; 68:175–183.

Larkum M. A cellular mechanism for cortical associations: an organizing principle for the cerebral cortex; 2013.

Lee RX, Huang JJ, Huang C, Tsai ML, Yen CT. Collateral projections from vestibular nuclear and inferior olivary neurons to lobules I/II and IX/X of the rat cerebellar vermis: a double retrograde labeling study. European Journal of Neuroscience. 2014; 40:2811–21.

Lee RX, Huang JJ, Huang C, Tsai ML, Yen CT. Plasticity of cerebellar Purkinje cells in behavioral training of body balance control; 2015.

Li Y, Zhong W, Wang D, Feng Q, Liu Z, Zhou J. Serotonin neurons in the dorsal raphe nucleus encode reward signals. Nat Commun. 2016; 7:10503.

Lister RG. The use of a plus-maze to measure anxiety in the mouse. Psychopharmacology. 1987; 92(2):180–185.

Mataix-Cols D, Cruz LFDL, Monzani B, Rosenfield D, Andersson E, Pérez-Vigil A, et al. D-Cycloserine Augmentation of Exposure-Based Cognitive Behavior Therapy for Anxiety, Obsessive-Compulsive, and Posttraumatic Stress Disorders: A Systematic Review and Meta-analysis of Individual Participant Data. JAMA psychiatry. 2017; 74:501–510.

Matias S, Lottem E, Dugue GP, Mainen ZF. Activity patterns of serotonin neurons underlying cognitive flexibility. Elife. 2017; 6:20552.

McAllister DE, McAllister WR. Incubation of fear: An examination of the concept. Journal of Experimental Research. 1967; in Personality .

McFarlane AC. The long-term costs of traumatic stress: intertwined physical and psychological consequences. World Psychiatry. 2010; 9(1):3–10.

McHugh PR, Treisman G. PTSD: A problematic diagnostic category. Journal of anxiety disorders. 2007; 21(2):211–222.

McIntyre DAN, Kelly ME. The parahippocampal cortices and kindling. Annals of the New York Academy of Sciences. 2000; 911(1):343–354.

McIntyre DC. The kindling phenomenon. In: *Models of Seizures and Epilepsy*; 2005. p. 351–363.

Miczek KA, O'donnell, M J. Intruder-evoked aggression in isolated and nonisolated mice: effects of psychomotor stimulants and L-dopa. Psychopharmacology. 1978; 57:47–55.

Mori S. Introduction to diffusion tensor imaging. Elsevier; 2007.

Mostoufi S, Godfrey KM, Ahumada SM, Hossain N, Song T, Wright LJ, et al. Pain sensitivity in posttraumatic stress disorder and other anxiety disorders: a preliminary case control study. Annals of general psychiatry. 2014; 13:31.

Murugan M, Jang HJ, Park M, Miller EM, Cox J, Taliaferro JP, et al. Combined social and spatial coding in a descending projection from the prefrontal cortex. Cell. 2017; 171(7):1663–1677.

Nadler JJ, Moy SS, Dold G, Trang D, Simmons N, Perez A, et al. Automated apparatus for quantitation of social approach behaviors in mice. Genes, Brain and Behavior. 2004; 3(5):303–314.

Okuyama T, Kitamura T, Roy DS, Itohara S, Tonegawa S. Ventral CA1 neurons store social memory. Science. 2016; 353:1536–1541.

Otabi H, Goto T, Okayama T, Kohari D, Toyoda A. The acute social defeat stress and nest-building test paradigm: A potential new method to screen drugs for depressive-like symptoms. Behavioural Processes. 2017; 135:71–75.

Pai A, Suris AM, North CS. Posttraumatic Stress Disorder in the DSM-5: Controversy, Change, and Conceptual Considerations. Behavioral Sciences. 2017; 7:7.

Pamplona F, Henes K, Micale V, Mauch C, Takahashi R, Wotjak C. Prolonged fear incubation leads to generalized avoidance behavior in mice. Journal of psychiatric research. 2011; 45:354–360.

Pavić L, Gregurek R, Radoš M, Brkljačić B, Brajković L, Šimetin Pavić I, et al. Smaller right hippocampus in war veterans with posttraumatic stress disorder. Psychiatry Research: Neuroimaging. 2007; 154(2):191–198.

Pellow S, Chopin P, File SE, Briley M. Validation of open: closed arm entries in an elevated plus-maze as a measure of anxiety in the rat. Journal of neuroscience methods. 1985; 14:149–167.

Pessoa L. On the relationship between emotion and cognition. Nature reviews neuroscience. 2008; 9(2):148.

Philbert J, Pichat P, Beeske S, Decobert M, Belzung C, Griebel G. Acute inescapable stress exposure induces long-term sleep disturbances and avoidance behavior: a mouse model of post-traumatic stress disorder. (PTSD) Behavioural brain research. 2011; 221:149–154.

Ramos A. Animal models of anxiety: do I need multiple tests?; 2008.

Rau V, DeCola JP, Fanselow MS. Stress-induced enhancement of fear learning: An animal model of post-traumatic stress disorder. Neurosci Biobehav Rev. 2005; 29(1207):1223.

Remedios R, Kennedy A, Zelikowsky M, Grewe BF, Schnitzer MJ, Anderson DJ. Social behaviour shapes hypothalamic neural ensemble representations of conspecific sex. Nature. 2017; 550(7676):388.

Roome CJ, Kuhn B. Simultaneous dendritic voltage and calcium imaging and somatic recording from Purkinje neurons in awake mice. Nature communications. 2018; 9(1):3388.

Russell PA, Williams DI. Effects of repeated testing on rats' locomotor activity in the open-field. In: *Animal behaviour*, vol. 21; 1973. p. 109–111.

Sandi C, Haller J. Stress and the social brain: behavioural effects and neurobiological mechanisms. Nature Reviews Neuroscience. 2015; 16:290–304.

Schnyder U, Cloitre M. Evidence based treatments for trauma-related psychological disorders: A practical guide for clinicians. Springer; 2015.

Shin LM, Rauch SL, Pitman RK. Amygdala, medial prefrontal cortex, and hippocampal function in PTSD. Annals of the New York Academy of Sciences. 2006; 1071(1):67–79.

Sial OK, Warren BL, Alcantara LF, Parise EM, Bolaños-Guzmán CA. Vicarious social defeat stress: Bridging the gap between physical and emotional stress. Journal of neuroscience methods. 2016; 258:94–103.

Siegmund A, Wotjak CT. Toward an animal model of posttraumatic stress disorder; 2006.

Sillivan SE, Joseph NF, Jamieson S, King ML, Chévere-Torres I, Fuentes I, et al. Susceptibility and resilience to posttraumatic stress disorder–like behaviors in inbred mice. Biological psychiatry. 2017; 82(12):924–933.

Smith ML, Hostetler CM, Heinricher MM, Ryabinin AE. Social transfer of pain in mice. Science advances. 2016; 2:1600855.

Takahashi A, Lee RX, Iwasato T, Itohara S, Arima H, Bettler B, et al. Glutamate input in the dorsal raphe nucleus as a determinant of escalated aggression in male mice. Journal of Neuroscience. 2015; 35:6452–6463.

Tononi G, Boly M, Massimini M, Koch C. Integrated information theory: from consciousness to its physical substrate. Nature Reviews Neuroscience. 2016; 17:450.

Tovote P, Fadok JP, Lüthi A. Neuronal circuits for fear and anxiety. Nature Reviews Neuroscience. 2015; 16:317–331.

Tsuda MC, Ogawa S. Long-lasting consequences of neonatal maternal separation on social behaviors in ovariectomized female mice. PLoS One. 2012; 7(3):33028.

Tsuda MC, Yeung HM, Kuo J, Usdin TB. Incubation of fear is regulated by TIP39 peptide signaling in the medial nucleus of the amygdala. Journal of Neuroscience. 2015; 35:12152–12161.

Voikar V, Vasar E, Rauvala H. Behavioral alterations induced by repeated testing in C57BL/6J and 129S2/Sv mice: implications for phenotyping screens. Genes, Brain and Behavior. 2004; 3(1):27–38.

Walf AA, Frye CA. The use of the elevated plus maze as an assay of anxiety-related behavior in rodents. Nature protocols. 2007; 2(2):322.

Walton JL, Cuccurullo LAJ, Raines AM, Vidaurri DN, Allan NP, Maieritsch KP, et al. Sometimes less is more: establishing the core symptoms of PTSD. Journal of traumatic stress. 2017; 30(3):254–258.

Warren BL, Vialou VF, Iñiguez SD, Alcantara LF, Wright KN, Feng J, et al. Neurobiological sequelae of witnessing stressful events in adult mice. Biological psychiatry. 2013; 73:7–14.

Yang T, Yang CF, Chizari MD, Maheswaranathan N, Burke KJ, Borius M, et al. Social control of hypothalamus-mediated male aggression. Neuron. 2017; 95(4):955–970.

Yehuda R, Hoge CW, McFarlane AC, Vermetten E, Lanius RA, Nievergelt CM, et al. Post-traumatic stress disorder. Nature Reviews Disease Primers. 2015; 1:15057.

Yu YQ, Barry DM, Hao Y, Liu XT, Chen ZF. Molecular and neural basis of contagious itch behavior in mice. Science. 2017; 355(6329):1072–1076.

Zelikowsky M, Hui M, Karigo T, Choe A, Yang B, Blanco MR, et al. The Neuropeptide Tac2 Controls a Distributed Brain State Induced by Chronic Social Isolation Stress. Cell. 2018; 173(5):1265–1279.

Zoladz PR, Diamond DM. Current status on behavioral and biological markers of PTSD: a search for clarity in a conflicting literature. Neuroscience & Biobehavioral Reviews. 2013; 37:860–895.